Activation of C_2H_6, C_3H_8, and c-C_3H_6 by Gas-Phase Rh^+ and the Thermochemistry of Rh−Ligand Complexes

Yu-Min Chen[†] and P. B. Armentrout*

Contribution from the Department of Chemistry, University of Utah, Salt Lake City, Utah 84112

Received March 22, 1995[⊗]

Abstract: The reactions of Rh^+ with C_2H_6, C_3H_8, and c-C_3H_6 at hyperthermal energies have been studied by using guided ion beam mass spectrometry. If is found that dehydrogenation is efficient and the dominant process at low energies in all three reaction systems. At high energies, C−H cleavage processes dominate the product spectrum for the reactions of Rh^+ with ethane and propane. C−C bond cleavage is a dominant process in the cyclopropane system. The reactions of Rh^+ are compared with those of Co^+ and the differences in behavior and mechanism are discussed in some detail. Modeling of the endothermic reaction cross sections yields the 0 K bond dissociation energies (in eV) of $D_0(Rh-H) = 2.42 \pm 0.06$, $D_0(Rh^+-C) = 4.25 \pm 0.18$, $D_0(Rh^+-CH) = 4.60 \pm 0.12$, $D_0(Rh^+-CH_2) = 3.69 \pm 0.08$, $D_0(Rh^+-CH_3) = 1.47 \pm 0.06$, $D_0(Rh^+-C_2H_2) = 1.67 \pm 0.03$, $D_0(Rh^+-C_2H_5) = 1.80 \pm 0.18$, and $D_0(Rh^+-C_3H_4) = 2.3 \pm 0.2$ and set lower limits of $D_0(Rh^+-C_2H_4) > 1.34$ and $D_0(Rh^+-C_3H_6) > 1.22$ eV.

Introduction

Considerable research has been done to study the reactions of the first-row transition-metal ions (M^+) with small hydrocarbons.[1,2] Such studies provide insight into the electronic requirements for the M^+ activation of C−H and C−C bonds,[2,3,4,5] periodic trends in the reactivity,[1,2] and metal−hydrogen and metal−carbon bond dissociation energies (BDEs).[6,7] The thermochemistry obtained from these studies is of obvious fundamental interest and also has implications in understanding a variety of catalytic reactions involving transition-metal systems.[8] Comparable studies are less extensive for the second-row transition-metal cations, although there are a number of studies in the literature.[9−15] In order to provide more detailed information on such systems, an ongoing project in our laboratory is to use guided ion beam mass spectrometry to systematically study the activation of small hydrocarbons by the second-row transition-metal cations. Elsewhere, we have studied the activation of several small hydrocarbons by Ag^+ and of methane by Rh^+.[16,17] In this work, we report additional studies of Rh^+ and describe its reactions with ethane, propane, and cyclopropane.

One of the challenging problems in the study of alkane activation by transition-metal ions is to determine the reaction mechanism. Previously, Byrd and Freiser[10] have studied the reactions of Rh^+ with several alkanes at thermal energy by using Fourier transform mass spectrometry (FTMS). Dehydrogenation was found to be the major process in all reaction systems. These authors postulated that the reaction mechanisms involved Rh^+ insertion into the C−H bond as the initial step followed by β-H transfer and reductive elimination of H_2. Later, Beauchamp and co-workers[12,13] studied the reactions of Rh^+ with alkanes by using ion beam techniques, but focused largely on the exothermic processes. Their observations and proposed mechanisms are essentially the same as those of Byrd and Freiser. Neither study provides detailed results for endothermic processes in these reaction systems, such as for processes involving C−C bond cleavage with the exception of formation of $RhCH_3^+$ in the ethane system.[13] In the present study, we investigate the reactions of Rh^+ with three hydrocarbons over a wide range of kinetic energies, examining both endothermic and exothermic processes and thus providing mechanistic information complementary to the previous work.

A particular reason for examining the endothermic reactions in detail is to determine accurate thermochemistry for rhodium−hydrogen and various rhodium−carbon species. The available information in the literature is collected in Table 1. Previously, bond dissociation energies (BDEs) for RhH^+, RhH, and $RhCH_3^+$

[†] Present address: Department of Chemistry, MIT, Cambridge, MA 02139.

[⊗] Abstract published in *Advance ACS Abstracts*, September 1, 1995.

(1) Allison, J. *Prog. Inorg. Chem.* **1986**, *34*, 627. Squires, R. R. *Chem. Rev.* **1987**, *87*, 623. *Gas Phase Inorganic Chemistry*; Russell, D. H., Ed.; Plenum: New York, 1989. Eller, K.; Schwarz, H. *Chem. Rev.* **1991**, *91*, 1121.

(2) For reviews, see: Armentrout, P. B. In *Selective Hydrocarbon Activation: Principles and Progress*; Davies, J. A., Watson, P. L., Greenberg, A., Liebman, J. F., Eds.; VCH: New York, 1990; p 467. Armentrout, P. B. In *Gas Phase Inorganic Chemistry*; Russell, D. H., Ed.; Plenum: New York, 1989; p 1. Armentrout, P. B.; Beauchamp, J. L. *Acc. Chem. Res.* **1989**, *22*, 315.

(3) For reviews, see: Armentrout, P. B. *Science* **1991**, *251*, 175. Armentrout, P. B. *Annu. Rev. Phys. Chem.* **1990**, *41*, 313.

(4) Weisshaar, J. C. *Adv. Chem. Phys.* **1992**, *82*, 213. Weisshaar, J. C. *Acc. Chem. Res.* **1993**, *26*, 213.

(5) van Koppen, P. A. M.; Kemper, P. R.; Bowers, M. T. *J. Am. Chem. Soc.* **1992**, *114*, 1083, 10941. van Koppen, P. A. M.; Kemper, P. R.; Bowers, M. T. *Organometallic Ion Chemistry*; Freiser, B. S., Ed.; Kluwer: Dordrect, 1995; in press.

(6) (a) Armentrout, P. B.; Kickel, B. L. In *Organometallic Ion Chemistry*; Freiser, B. S., Ed.; Kluwer: Dordrecht, 1995; pp 1−45. (b) Armentrout, P. B.; Clemmer, D. E. In *Energetics of Organometallic Species*; Simoes, J. A. M., Beauchamp, J. L., Eds.; Kluwer: Dordrect, 1992; p 321. (c) Armentrout, P. B. *ACS Symp. Ser.* **1990**, *428*, 18. (d) Armentrout, P. B.; Georgiadis, R. *Polyhedron* **1988**, *7*, 1573.

(7) *Organometallic Ion Chemistry*, Freiser, B. S., Ed.; Kluwer: Dordrect, 1995; in press.

(8) Crabtree, R. H. *Chem. Rev.* **1985**, *85*, 245.

(9) Sunderlin, L. S.; Armentrout, P. B. *J. Am. Chem. Soc.* **1989**, *111*, 3845. Sunderlin, L. S.; Armentrout, P. B. *Organometallics* **1990**, *9*, 1248.

(10) Byrd, G. D.; Freiser, B. S. *J. Am. Chem. Soc.* **1982**, *104*, 5944.

(11) Huang, Y.; Wise, M. B.; Jacobson, D. B.; Freiser, B. S. *Organometallics* **1987**, *6*, 346. Buckner, S. W.; MacMahon, T. J.; Byrd, G. D.; Freiser, B. S. *Inorg. Chem.* **1989**, *28*, 3511. Gord, J. R.; Freiser, B. S.; Buckner, S. W. *J. Chem. Phys.* **1989**, *91*, 7530. Ranasinghe, Y. A.; MacMahon, T. J.; Freiser, B. S. *J. Phys. Chem.* **1991**, *95*, 7721.

(12) Tolbert, M. A.; Mandich, M. L.; Halle, L. F.; Beauchamp, J. L. *J. Am. Chem. Soc.* **1986**, *108*, 5675.

(13) Mandich, M. L.; Halle, L. F.; Beauchamp, J. L. *J. Am. Chem. Soc.* **1984**, *106*, 4403.

(14) Schilling, J. B.; Beauchamp, J. L. *Organometallics* **1988**, *7*, 194.

(15) Blomberg, M. R. A.; Siegbahn, P. E. M.; Sevensson, M. *J. Phys. Chem.* **1994**, *98*, 2062.

(16) Chen, Y.-M.; Armentrout, P. B. *J. Phys. Chem.* **1995**, *99*, 11424.

(17) Chen, Y.-M.; Armentrout, P. B. *J. Phys. Chem.* **1995**, *99*, 10775.

0002-7863/95/1517-9291$09.00/0

Table 1. Rhodium−Ligand Bond Dissociation Energies (in eV) at 0 K[a]

bond	literature: expl	literature: theor	this work
Rh^+-H	1.78(0.13)[b,c]	1.51,[d] 1.80,[e] 1.82,[g] 1.77[h]	1.67(0.04)[f]
Rh−H	2.52(0.22)[b,i]	2.77[j,k]	2.42(0.06)
Rh^+-C	7.07(0.69)[b,l]		4.25(0.18)
Rh^+-CH	4.36(0.30)[b,m]		4.60(0.12)
Rh^+-CH_2	4.01(0.22)[b,n]	3.64(0.17)[o]	3.69(0.08)
	3.80(0.22)[b,m]	3.40,[g,p] 3.43(0.13)[h]	
Rh^+-CH_3	1.97(0.22)[b,c]	1.61,[k] 1.63,[g] 1.65[h]	1.47(0.06)
$Rh^+-C_2H_2$[r]		1.27[q]	1.67(0.03)
$Rh^+-C_2H_4$		1.78[h]	>1.34(0.01)
$Rh^+-C_2H_5$[r]		1.98[h]	1.80(0.18)
$Rh^+-C_3H_4$[r]			2.3(0.2)
$Rh^+-C_3H_6$			>1.22(0.01)

[a] Uncertainties in parentheses. [b] Original 298 K values are adjusted to 0 K by subtracting 0.039 eV = $3k_BT/2$ for RhH^+, RhC^+, and $RhCH^+$ and 0.064 eV = $5k_BT/2$ for $RhCH_3^+$ and $RhCH_2^+$. [c] Reference 13. [d] Reference 23. [e] Reference 24. [f] Reference 19. [g] Reference 26. [h] Reference 27. [i] Reference 18. [j] Reference 25. [k] Reference 28. [l] Reference 22. [m] Reference 21. [n] Reference 20. [o] Reference 31. [p] Reference 30. [q] Reference 33. [r] The ground state structure of this species is unclear, see text.

have been measured by using ion beam techniques,[13,18,19] and those for $RhCH_2^+$, $RhCH^+$, and RhC^+ have been determined by using FTMS and photodissociation techniques.[20−22] In addition, theoretical calculations have been performed for the BDEs of cationic and neutral rhodium hydrides,[23−27] rhodium methyls,[26−29] rhodium methylenes,[26,27,30−32] and several $Rh^+-C_2H_x$ species.[27,33] As can be seen from Table 1, these previously measured BDEs generally have large uncertainties and are determined by only a single technique. In addition, there is a potential problem because the reactant ions (created by laser vaporization in the FTMS experiments and by surface ionization in the beam studies) could be in excited electronic states, and the accuracy of the BDEs depends on how the excitation energies are handled. In the present work, we remeasure these BDEs by determining the endothermic reaction thresholds for reactions of Rh^+ with the three hydrocarbons and also utilize similar results for reactions of Rh^+ with methane.[17] We use a dc-discharge flow tube ion source to produce Rh^+ ions that are believed to be in the ^3F electronic ground state term, and primarily in the lowest spin−orbit level, $^3F_4$.[19,34] Thus, the threshold measurements have fewer complexities associated with the presence of excited state ions.

Experimental Section

General Procedures. The guided ion beam instrument on which these experiments were performed has been described in detail previously.[35,36] Rh^+ ions are created in a flow tube source, described below. The ions are extracted from the source, accelerated, and focused into a magnetic sector momentum analyzer for mass analysis. Mass-selected ions are slowed to a desired kinetic energy and focused into an octopole ion guide that radially traps the ions.[37] The octopole passes through a static gas cell containing the neutral reactant. Gas pressures in the cell are kept sufficiently low (usually less than 0.2 mTorr) that multiple ion−molecule collisions are improbable. Except where noted, all results reported here are due to single bimolecular encounters, as verified by pressure dependent studies. Product and unreacted beam ions are contained in the guide until they drift out of the gas cell where they are focused into a quadrupole mass filter for mass analysis and then detected by a high voltage scintillation detector. Ion intensities are converted to absolute cross sections as described previously.[35] Uncertainties in absolute cross sections are estimated to be ±20%.

Laboratory ion energies (lab) are converted to energies in the center-of-mass frame (CM) by using the following formula, $E_{CM} = E_{lab}m/(m + M)$, where M and m are the ion and neutral reactant masses, respectively. Two effects broaden the cross section data: the kinetic energy distribution of the ion and the thermal motion of the neutral reactant gas (Doppler broadening).[38] The distribution of the ion kinetic energy and absolute zero of the energy scale are determined by using the octopole beam guide as a retarding potential analyzer.[35] The distribution of ion energies, which is independent of energy, is nearly Gaussian and has an average full width at half maximum (fwhm) of ~0.45 eV (lab). The Doppler broadening has a width of $\sim 0.45E_{CM}^{1/2}$ for the reactions of Rh^+ with the three hydrocarbons.[38] Uncertainties in the absolute energy scale are ±0.05 eV (lab).

Ion Source. Rh^+ ions are produced in a dc-discharge flow tube (FT) source.[36] The flow gases used in this experiment are ~90% He and ~10% Ar, maintained at a total pressure of 0.5−0.7 Torr at ambient temperatures. A dc discharge at a voltage of ~2.5 kV is used to ionize argon and then accelerate these ions into a tantalum cathode with a cavity containing rhodium chloride, thereby sputtering Rh^+ ions. The ions are swept down a meter long flow tube and undergo $\sim 10^5$ collisions with the He and Ar flow gasses. The Rh^+ ions created under these flow tube conditions have been shown to have an electronic temperature <1100 K, which has been conservatively assigned as 700 ± 400 K, as discussed in detail elsewhere.[19] No evidence for excited electronic states is found in the present or three other studies,[17,19,34] and the thermochemistry derived here is consistent with this assignment. At 1100 K, 99.998% of the Rh^+ ions are in the ^3F electronic ground state term, 96.3% are in the lowest spin−orbit level, $^3F_4$, and the average electronic energy is 0.012 eV.

Data Analysis. Endothermic reaction cross sections are modeled by using eq 1,[39]

$$\sigma(E) = \sigma_0 \sum_i g_i (E + E_i + E_{int} - E_0)^n / E \qquad (1)$$

which involves an explicit sum of the contributions of individual electronic states of the Rh^+ reactant, denoted by i, having energies E_i and populations g_i, where $\sum g_i = 1$. Here, σ_0 is an energy-independent scaling factor, E is the relative kinetic energy of the ions, E_0 is the 0 K reaction threshold, and n is an adjustable parameter. Equation 1 also takes into account the internal energy of the neutral reactant, E_{int}. At 305 K (the nominal temperature of the octopole), the average internal energy for each neutral reactant is the average rotational energy, $3k_BT/2$

(18) Tolbert, M. A.; Beauchamp, J. L. *J. Phys. Chem.* **1986**, *90*, 5015.
(19) Chen, Y.-M.; Elkind, J. L.; Armentrout, P. B. *J. Phys. Chem.* **1995**, *99*, 10438.
(20) Jacobson, D. B.; Freiser, B. S. *J. Am. Chem. Soc.* **1985**, *107*, 5870.
(21) Hettich, R. L.; Freiser, B. S. *J. Am. Chem. Soc.* **1987**, *109*, 3543.
(22) Jacobson, D. B.; Byrd, G. D.; Freiser, B. S. *Inorg. Chem.* **1984**, *23*, 553.
(23) Schilling, J. B.; Goddard, W. A., III; Beauchamp, J. L. *J. Am. Chem. Soc.* **1987**, *109*, 5565.
(24) Pettersson, L. G. M.; Bauschlicher, C. W., Jr.; Langhoff, S. R.; Partridge, H. *J. Chem. Phys.* **1987**, *87*, 481.
(25) Langhoff, S. R.; Pettersson, L. G. M.; Bauschlicher, C. W., Jr. *J. Chem. Phys.* **1987**, *86*, 268.
(26) Musaev, D. G.; Morokuma, K. *Isr. J. Chem.* **1993**, *33*, 307.
(27) Perry, J. K. Ph.D. Thesis, Caltech, 1994.
(28) Bauschlicher, C. W., Jr.; Langhoff, S. R.; Partridge, H.; Barnes, L. A. *J. Chem. Phys.* **1989**, *91*, 2399.
(29) Siegbahn, P. E. M. *J. Am. Chem. Soc.* **1994**, *116*, 7722.
(30) Musaev, D. G.; Koga, N.; Morokuma, K. *J. Phys. Chem.* **1993**, *97*, 4064.
(31) Bauschlicher, C. W., Jr.; Partridge, H.; Sheehy, J. A.; Langhoff, S. R.; Rosi, M. *J. Phys. Chem.* **1992**, *96*, 6969.
(32) Siegbahn, P. E. M. *Chem. Phys. Lett.* **1993**, *201*, 15.
(33) Sodupe, M.; Bauschlicher, C. W., Jr. *J. Phys. Chem.* **1991**, *95*, 8640.
(34) Chen, Y.-M.; Armentrout, P. B. *J. Chem. Phys.* **1995**, *103*, 618.
(35) Ervin, K. M.; Armentrout, P. B. *J. Chem. Phys.* **1985**, *83*, 166.
(36) Schultz, R. H.; Armentrout, P. B. *Int. J. Mass Spectrom. Ion Processes* **1991**, *107*, 29.
(37) Teloy, E.; Gerlich, D. *Chem. Phys.* **1974**, *4*, 417. Gerlich, D.; Diplomarbeit, University of Freiburg, Federal Republic of Germany, 1971. Gerlich, D. In *State-Selected and State-to-State Ion−Molecule Reaction Dynamics. Part 1. Experiment*; Ng, C.-Y., Baer, M., Eds.; *Adv. Chem. Phys.* **1992**, *82*, 1.
(38) Chantry, P. J. *J. Chem. Phys.* **1971**, *55*, 2746.
(39) Armentrout, P. B. In *Advances in Gas Phase Ion Chemistry*; Adams, N. G., Babcock, L. M., Eds.; JAI: Greenwich, 1992; Vol. 1, p 83.

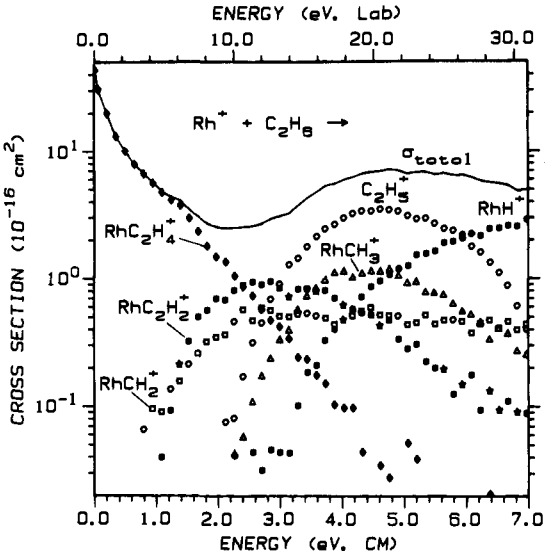

Figure 1. Cross sections for reactions of Rh^+ with C_2H_6 as a function of kinetic energy in the center-of-mass frame (lower axis) and laboratory frame (upper axis).

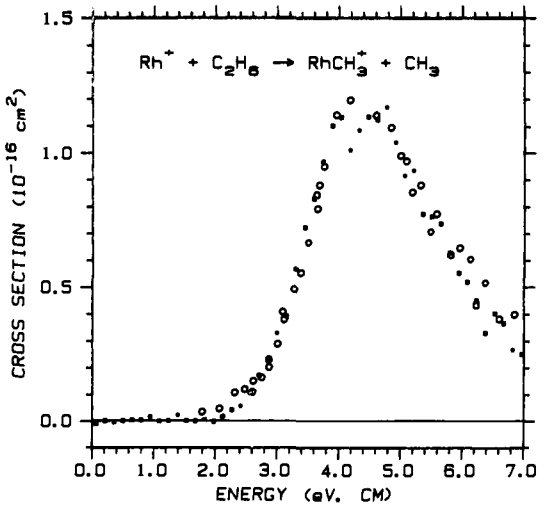

Figure 2. Cross sections for the reaction $Rh^+ + C_2H_6 \rightarrow RhCH_3^+ + CH_3$, process 4, as a function of kinetic energy in the center-of-mass frame. The solid squares show the present FT cross section data, and the open circles the previous SI cross section data (where a C_2D_6 reactant is used) from ref 13 scaled up by a factor of 1.5.

= 0.039 eV, plus its average vibrational energy. The average vibrational energies are 0.020, 0.050, and 0.017 eV for C_2H_6, C_3H_8, and c-C_3H_6, respectively, which are calculated from vibrational frequencies taken from Shimanouchi.[40] Before comparison with the data, eq 1 is convoluted with the kinetic energy distributions of the ion and neutral reactants.[35] The σ_0, n, and E_0 parameters are then optimized by using a nonlinear least-squares analysis to give the best reproduction of the data. Error limits for E_0 are calculated from the range of threshold values for different data sets over a range of acceptable n values, the uncertainty associated with the electronic temperature, and the absolute error in the energy scale.

Results

$Rh^+ + C_2H_6$. Ten ionic products are observed in the reaction of Rh^+ with C_2H_6. Figure 1 shows cross sections as a function of kinetic energy for the six major ionic products formed in reactions 2–7. For clarity, cross sections for the other four

$$Rh^+ + C_2H_6 \rightarrow RhH^+ + C_2H_5 \quad (2)$$

$$\rightarrow C_2H_5^+ + RhH \quad (3)$$

$$\rightarrow RhCH_3^+ + CH_3 \quad (4)$$

$$\rightarrow RhCH_2^+ + CH_4 \quad (5)$$

$$\rightarrow RhC_2H_4^+ + H_2 \quad (6)$$

$$\rightarrow RhC_2H_2^+ + 2H_2 \quad (7)$$

ionic products, $C_2H_3^+$, $RhCH^+$, RhC^+, and $RhC_2H_3^+$, are not shown in Figure 1. Their cross sections have magnitudes less than 0.4 Å^2 and apparent thresholds above 3 eV. As can be seen from Figure 1, the cross section for the dehydrogenation channel, reaction 6, decreases with increasing energy (approximately as $E^{-0.5}$ below 0.2 eV, as $E^{-0.7}$ from 0.2 to 1.4 eV, and much faster at higher energies), indicating an exothermic process. Compared to the Langevin–Gioumousis–Stevenson collision cross section,[41] we find this reaction is about 23% efficient below 0.2 eV. All other reactions exhibit reaction thresholds, consistent with previous studies[10,12] where $RhC_2H_4^+$ is the only ionic product observed at thermal and up to 2 eV of kinetic energies. Tolbert et al.[12] report magnitudes for the $RhC_2H_4^+$ product of 19 Å^2 at 0.5 eV and 1.0 Å^2 at 2.0 eV, in reasonable agreement with the present results. Differences between the previous ion beam results and the present results can probably be attributed to the higher sensitivity and better kinetic energy calibration of the present experiment.

Figure 1 shows that reactions 2, 3, 6, and 7, which involve C–H bond cleavage, dominate the product spectrum. The dehydrogenation channel, reaction 6, is the dominant process at low energies. At an energy near the onset of the $RhC_2H_2^+$ cross section, the $RhC_2H_4^+$ cross section begins to decline more rapidly, suggesting that it decomposes to $RhC_2H_2^+ + H_2$ in the overall reaction 7. At high energies, formation of the ionic and neutral metal hydrides, reactions 2 and 3 are the dominant processes. The $C_2H_5^+ + RhH$ cross section shows an apparent threshold lower than the $RhH^+ + C_2H_5$ cross section. Because the only difference between the two reactions is the location of the positive charge, this threshold difference is a direct indication of the relative ionization energies (IE), namely, IE(C_2H_5) < IE(RhH). At the highest energies, the $C_2H_5^+$ cross section declines rapidly. This is anomalous behavior caused by incomplete collection of this product because it has a small velocity in the laboratory frame.

The C–C bond cleavage reaction that leads to the formation of $RhCH_3^+$, reaction 4, has a small cross section magnitude relative to those for the C–H bond cleavage reactions (Figure 1). Our results for this process are in good agreement with those of Mandich et al.[13] as shown in Figure 2, although our absolute cross section is 50% larger, a difference that is within the combined experimental errors. The $RhCH_3^+$ cross section rises from an apparent threshold of about 2 eV and reaches a maximum near 4 eV. Above this energy, the cross section begins to decline due to dissociation of $RhCH_3^+$ to $Rh^+ + CH_3$, an overall reaction in which ethane dissociates into two methyl groups. The peak position agrees with the thermodynamic threshold for this dissociation, $D_0(CH_3–CH_3) = 3.812 \pm 0.007$ eV (Table 2).

The elimination of methane in reaction 5 is a process that involves both C–C and C–H bond cleavages. The magnitude of the $RhCH_2^+$ cross section is small relative to other processes

(40) Shimanouchi, T. *Tables of Molecular Vibrational Frequencies Consolidated*; National Bureau of Standards: Washington, DC, 1972; Vol. I, NSRDS-NBS 39.

(41) Gioumousis, G.; Stevenson, D. P. *J. Chem. Phys.* **1958**, *29*, 292.

(Figure 1), even though it has the lowest apparent threshold among all endothermic processes.

$Rh^+ + C_3H_8$. Fourteen ionic products are observed in the reaction of Rh^+ with C_3H_8. Figure 3 shows cross sections as a function of kinetic energy for the 12 ionic products formed in reactions 8–19. The other two ionic products, RhC^+ and $RhCH^+$, have cross sections with thresholds above 4.5 eV and magnitudes less than 0.2 Å^2. Our results are in good agreement with those of Tolbert et al.,[12] both in terms of the absolute cross sections and the product branching ratios reported at 0.5 and 2.0 eV, although we again observe minor products not mentioned in the previous study because of the higher sensitivity of the present experiment. As can be seen from Figure 3, the dehydrogenation channel, reaction 12, is the only exothermic reaction, in agreement with the findings of Tolbert et al.[12] In contrast, the FTMS study of Byrd and Freiser[10] yielded $RhC_3H_6^+$ as the major ionic product (94%) and $RhC_2H_4^+$ as a minor ionic product (6%). In the present study, these products constitute >99.95% and <0.05%, respectively, of the total product ion intensity observed at our lowest energy of ~0.1 eV. This difference suggests that the laser desorption ion source used in the FTMS study probably created Rh^+ ions in excited states or that the Rh^+ ions are kinetically excited, as also suggested by Tolbert et al.[12]

$$Rh^+ + C_3H_8 \rightarrow RhH^+ + C_3H_7 \quad (8)$$

$$\rightarrow C_3H_7^+ + RhH \quad (9)$$

$$\rightarrow C_3H_5^+ + H_2 + RhH \quad (10)$$

$$\rightarrow C_2H_3^+ + CH_4 + RhH \quad (11)$$

$$\rightarrow RhC_3H_6^+ + H_2 \quad (12)$$

$$\rightarrow RhC_3H_4^+ + 2H_2 \quad (13)$$

$$\rightarrow RhC_2H_4^+ + CH_4 \quad (14)$$

$$\rightarrow RhC_2H_2^+ + H_2 + CH_4 \quad (15)$$

$$\rightarrow RhCH_2^+ + C_2H_6 \quad (16)$$

$$\rightarrow RhCH_3^+ + C_2H_5 \quad (17)$$

$$\rightarrow RhC_2H_5^+ + CH_3 \quad (18)$$

$$\rightarrow RhC_2H_3^+ + H_2 + CH_3 \quad (19)$$

The dominant processes in the propane system are again those involving C–H bond cleavage, reactions 9, 12, and 13. The dehydrogenation channel, reaction 12, is dominant at low energies and follows the Langevin–Gioumousis–Stevenson collision cross section,[41] below 0.6 eV. The $RhC_3H_6^+$ cross section falls off more rapidly as the $RhC_3H_4^+$ cross section rises, a consequence of the decomposition of $RhC_3H_6^+$ into $RhC_3H_4^+ + H_2$ in the overall reaction 13. The formation of $RhH + C_3H_7^+$, reaction 9, is the dominant process at high energies. The cross section of this reaction has an apparent threshold much smaller than that of reaction 8, formation of $RhH^+ + C_3H_7$, implying that $IE(C_3H_7) < IE(RhH)$. The $C_3H_7^+$ cross section declines at high energies by decomposition into $C_3H_5^+ + H_2$ and $C_2H_3^+ + CH_4$ in the overall reactions 10 and 11, respectively.

Table 2. Literature Thermochemistry at 0 K

species	Δ_fH_0 (eV)	IE (eV)
H	2.239[a]	
C	7.371(0.005)[a]	
CH	6.145(0.018)[b]	
CH_2	4.02(0.03)[c]	
CH_3	1.553(0.004)[d]	9.843(0.002)[d]
CH_4	−0.688(0.004)[e,f]	
C_2H_2	2.371(0.007)[e,f]	
CH_2C	4.43(0.17)[b]	
C_2H_4	0.632(0.004)[e,f]	
$CHCH_3$	3.4(0.1)[g]	
C_2H_5	1.368(0.022)[d,h]	8.117(0.008)[d]
C_2H_6	−0.707(0.004)[e,i]	
CH_3CCH	2.004(0.008)[e,i]	
CH_2CCH_2	2.067(0.012)[e,i]	
CH_2CHCH_2	1.89(0.09)[d]	8.13(0.02)[j]
c-C_3H_5	3.04(0.01)[k]	8.18(0.03)[l]
c-C_3H_6	0.730(0.006)[e,m]	
C_3H_6	0.363(0.008)[e,n]	
1-C_3H_7	1.17(0.02)[l]	8.09(0.01)[l]
2-C_3H_7	1.117(0.026)[d]	7.36(0.02)[l]
C_3H_8	−0.854(0.005)[e,n]	

[a] Chase, M. W.; Davies, C. A.; Downey, J. R.; Frurip, D. J.; McDonald, R. A.; Syverud, A. N. *J. Phys. Chem. Ref. Data* **1985**, *14*, Suppl. No. 1 (JANAF Tables). [b] Ervin, K. M.; Gronert, S.; Barlow, S. E.; Gilles, M. K.; Harrison, A. G.; Bierbaum, V. M.; DePuy, C. H.; Lineberger, W. C.; Ellison, G. B. *J. Am. Chem. Soc.* **1990**, *112*, 5750. [c] Leopold, D. G.; Murray, K. K.; Stevens Miller, A. E.; Lineberger, W. C. *J. Chem. Phys.* **1985**, *83*, 4849. [d] Berkowitz, J.; Ellison, G. B.; Gutman, D. *J. Phys. Chem.* **1994**, *98*, 2744. [e] Δ_fH_{298} value from: Pedley, J. B.; Naylor, R. D.; Kirby, S. P. *Thermochemical Data of Organic Compounds*, 2nd ed.; Chapman and Hall: New York, 1986. [f] Adjusted to 0 K by using information in footnote *a*. [g] Reference 50. Pople, J. A.; Raghavachari, K.; Frisch, M. J.; Binkly, J. S.; Schelyer, P. v. R. *J. Am. Chem. Soc.* **1983**, *105*, 6389. Trinquier, G. *J. Am. Chem. Soc.* **1990**, *112*, 2130. [h] Seakins, P. W.; Pilling, M. J.; Niiranen, J. T.; Gutman, D.; Krasnoperov, L. N. *J. Phys. Chem.* **1992**, *96*, 9847. [i] Adjusted to 0 K by using information from: Wagman, D. D.; Evans, W. H.; Parker, V. B.; Schumm, R. H.; Halow, I.; Bailey, S. M.; Churney, K. L.; Nuttall, R. L. *J. Phys. Chem. Ref. Data* **1982**, *11*, Suppl. No. 2. [j] Houle, F. A.; Beauchamp, J. L. *J. Am. Chem. Soc.* **1978**, *100*, 3290. [k] Estimated, assuming ideal gas behavior, from Δ_fH_{298} (McMillen, D. F.; Golden, D. M. *Annu. Rev. Phys. Chem.* **1982**, *33*, 493) and the vibrational frequencies for c-C_3H_6 (ref 40). [l] Reference 51. [m] Adjusted to 0 K by using information from: Dorofeeva, O. V.; Gurvich, L. V.; Jorish, V. S. *J. Phys. Chem. Ref. Data* **1986**, *15*, 437. [n] Adjusted to 0 K by using the information in: *Handbook of Chemistry and Physics*, 71st ed.; Lide, D. R., Ed.; CRC Press: Boca Raton, 1990; pp 5–74.

The cross section for the elimination of methane, reaction 14, rises from an onset near zero, reaches a maximum at ~2 eV, and then declines rapidly. Part of this decline can be attributed to the decomposition of $RhC_2H_4^+$ into $RhC_2H_2^+ + H_2$ in the overall reaction 15; however, we note that the sum of the cross sections for reactions 14 and 15 still has a maximum near 2 eV. This is possibly because of competition with reactions 16 and 18, given that their cross sections have onsets near 2 eV (Figure 3). The cross section for reaction 15 exhibits two features. One appears at low energies with an apparent threshold of ~0.4 eV and reaches a maximum at ~1 eV, and the other feature appears at high energies with a larger cross section. It was verified that these cross section features are reproducible and do not exhibit any C_3H_8 pressure dependence, eliminating the possibility that they are due to secondary reactions.

Although the $RhCH_2^+$ cross section (Figure 3b) appears to rise from a threshold just below 2 eV, a very careful look at the data finds that this cross section has a small tail at lower energies, Figure 4. This small tail has an apparent threshold of ~0.5 eV, and its magnitude is less than 0.01 Å^2.

Figure 3 shows that C–C bond cleavage processes, reactions 17 and 18, have cross sections smaller than those for C–H bond

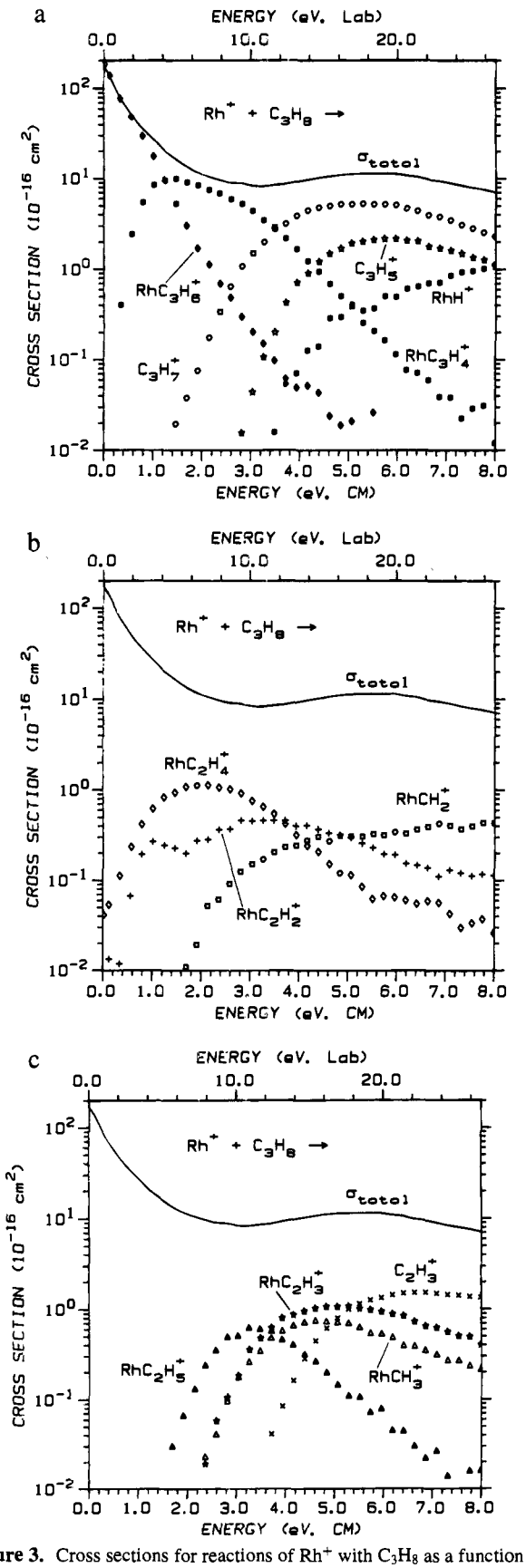

Figure 3. Cross sections for reactions of Rh^+ with C_3H_8 as a function of kinetic energy in the center-of-mass frame (lower axis) and laboratory frame (upper axis). Part a shows results for C−H bond cleavage reactions 8−10, 12, and 13; part b, for reactions 14−16; and part c, for reactions 11, 17−19. The full lines in parts a−c show the total reaction cross section.

cleavage processes, similar to the observations in the C_2H_6 system. The $RhC_2H_5^+$ cross section reaches a maximum below

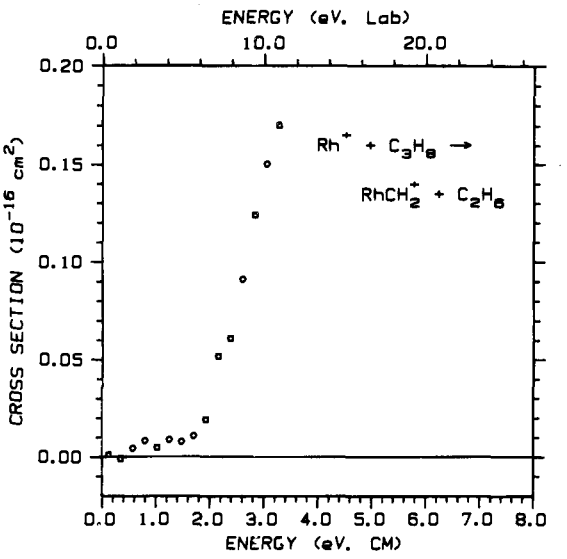

Figure 4. Threshold region for the cross section for the reaction $Rh^+ + C_3H_8 \rightarrow RhCH_2^+ + C_2H_6$, process 16, as a function of kinetic energy in the center-of-mass frame (lower axis) and laboratory frame (upper axis).

the thermodynamic threshold for dissociation of $RhC_2H_5^+ + CH_3$ into $Rh^+ + C_2H_5 + CH_3$, $D_0(C_2H_5-CH_3) = 3.77 \pm 0.02$ eV (Table 2). Thus, the decline of the $RhC_2H_5^+$ cross section must be partially due to its decomposition into $RhC_2H_3^+ + H_2$ in the overall reaction 19. The $RhCH_3^+$ cross section reaches a maximum at ~4.6 eV due to the dissociation of $RhCH_3^+$ into $Rh^+ + CH_3$, higher than the thermodynamic threshold at $D_0(C_2H_5-CH_3)$. This indicates that some of the excess internal energy, necessary for the decomposition of $RhCH_3^+$, is carried away by the C_2H_5 neutral product.

Rh^+ + c-C_3H_6. Twelve ionic products are observed in the reaction of Rh^+ with c-C_3H_6. Figure 5 shows cross sections as a function of kinetic energy for the ten ionic products formed in reactions 20−29. Two other ionic products, $RhCH^+$ and

$$Rh^+ + c\text{-}C_3H_6 \rightarrow RhH^+ + C_3H_5 \quad (20)$$

$$\rightarrow C_3H_5^+ + RhH \quad (21)$$

$$\rightarrow C_3H_3^+ + H_2 + RhH \quad (22)$$

$$\rightarrow RhC_3H_4^+ + H_2 \quad (23)$$

$$\rightarrow RhC_3H_2^+ + 2H_2 \quad (24)$$

$$\rightarrow RhC_2H_2^+ + CH_4 \quad (25)$$

$$\rightarrow RhCH_2^+ + C_2H_4 \quad (26)$$

$$\rightarrow RhC^+ + H_2 + C_2H_4 \quad (27)$$

$$\rightarrow RhC_2H_4^+ + CH_2 \quad (28)$$

$$\rightarrow RhC_2H_3^+ + CH_3 \quad (29)$$

$RhC_3H_6^+$, are not shown. The $RhCH^+$ cross section has an apparent threshold of 4.5 eV and its magnitude is less than 0.5 Å^2. The $RhC_3H_6^+$ cross section exhibits exothermic behavior and its magnitude is about 30 times smaller than the $RhC_3H_4^+$ cross section at a neutral reactant pressure of 0.16 mTorr. The

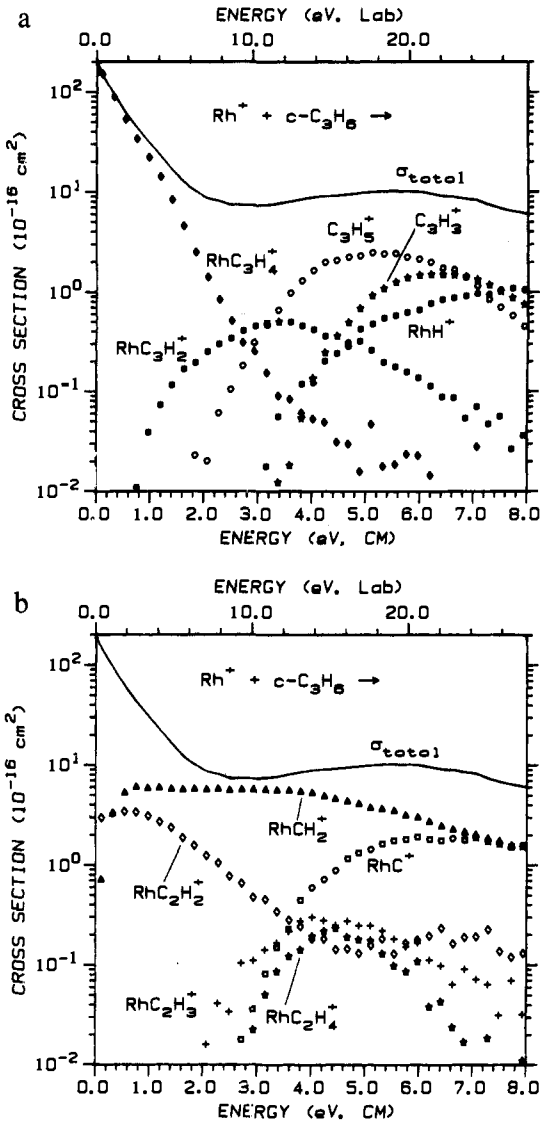

Figure 5. Cross sections for reactions of Rh^+ with c-C_3H_6 as a function of kinetic energy in the center-of-mass frame (lower axis) and laboratory frame (upper axis). Part a shows results for C−H bond cleavage reactions 20−24, and part b shows results for C−C bond cleavage reactions 25−29. The full lines in both parts show the total reaction cross section.

$RhC_3H_6^+$ ion is a collisionally stabilized complex as established by the linear pressure dependence of its cross section. We also observed $RhC_2H_4^+$ at energies below about 3 eV, but in this region, the cross section is pressure dependent, indicating that this ion is formed by an efficient, exothermic secondary reaction, $RhCH_2^+ + c\text{-}C_3H_6 \rightarrow RhC_2H_4^+ + C_2H_4$. The contribution of this process has been removed from Figure 5, which shows only processes corresponding to single ion−molecule collisions (pressure independent cross sections).

In their FTMS study of this system, Byrd and Freiser[10] observed $RhC_3H_6^+$ (6%), $RhC_3H_4^+$ (76%), $RhC_2H_4^+$ (3%), $RhC_2H_2^+$ (4%), and $RhCH_2^+$ (11%) at thermal energies. At our lowest kinetic energy, we observe a product distribution at zero pressure of $RhC_3H_4^+$ (97.9%), $RhC_2H_2^+$ (1.7%), and $RhCH_2^+$ (0.4%), respectively. We note that the distribution of the $RhC_3H_4^+$, $RhC_2H_2^+$, and $RhCH_2^+$ products observed by Byrd and Freiser is comparable to what we find at about 0.6 eV, again suggesting that the Rh^+ ions in the FTMS study are excited either translationally or electronically. As noted above, the amounts of $RhC_3H_6^+$ and $RhC_2H_4^+$ observed at low energies depend on the pressure of c-C_3H_6 and so a direct comparison between the present and the FTMS results cannot be made.

Figure 5 shows that the dehydrogenation channel, reaction 23, is the dominant process at low energies and follows the Langevin−Gioumousis−Stevenson collision cross section[41] below 0.3 eV. The double dehydrogenation channel, reaction 24, is observed to be an endothermic process with a cross section magnitude less than 0.5 Å^2. Formation of both ionic and neutral rhodium hydrides, reactions 20 and 21, is seen at high energies. The $C_3H_5^+$ cross section is much larger than the RhH^+ cross section, and also has an apparent threshold smaller than the latter, indicating that IE(C_3H_5) < IE(RhH). The $C_3H_3^+$ ion is observed at high energies due to the decomposition of $C_3H_5^+$ into $C_3H_3^+ + H_2$ in the overall reaction 22.

Unlike in the C_2H_6 and C_3H_8 reaction systems, the endothermic C−H bond cleavage reactions are no longer the dominant processes at high energies. Instead, the C−C bond cleavage reaction 26 is the dominant endothermic process through much of the experimental energy range studied. The $RhCH_2^+$ cross section rises rapidly from an apparent threshold near zero, levels out at about 6 Å^2 at low energies, and then begins to decrease at an energy near 4 eV due to the dissociation of $RhCH_2^+$ into $Rh^+ + CH_2$ and $RhC^+ + H_2$. These dissociation channels have thermodynamic thresholds of 3.92 ± 0.03 eV = $D_0(C_2H_4\text{−}CH_2)$ (Table 2) and 3.02 ± 0.18 eV (based on the thermochemistry measured below), respectively. The magnitude of the RhC^+ cross section is larger in this system than in the other three systems, consistent with the observation that its precursor, $RhCH_2^+$, has the largest cross section magnitude in the c-C_3H_6 system.

Formation of $RhC_2H_4^+$ in reaction 28 is another C−C bond cleavage process, although its cross section is much smaller than that for $RhCH_2^+$. This cross section declines at energies above ~4.4 eV, probably because of dissociation into $Rh^+ + C_2H_4$, which can begin at 3.92 ± 0.03 eV. $RhC_2H_3^+$ cannot be formed by H atom loss from $RhC_2H_4^+$ because its threshold is lower than that of $RhC_2H_4^+$. Thus, the neutral product must be CH_3, reaction 29, indicating substantial rearrangement. Figure 5 shows that the formation of $RhC_2H_2^+$ is relatively efficient at low energies and exhibits a finite cross section at our lowest energy. Thermochemical arguments (see below) establish that CH_4 is the neutral product, reaction 25. The $RhC_2H_2^+$ cross section declines above ~0.6 eV. This is probably because of dissociation to $Rh^+ + C_2H_2$, which can begin at 0.95 ± 0.01 eV, and because this channel competes with $RhCH_2^+$ formation.

Discussion

Thermochemical Results. The endothermic cross sections in each reaction system are analyzed in detail by using eq 1 as described in the Experimental Section. The optimized parameters obtained are summarized in Table 3. For some minor reaction channels in each reaction system, such analyses were not performed due to the poor quality of the data. From the thresholds measured, the BDEs for the rhodium−ligand product species observed in the reaction of Rh^+ + R−L can be calculated using eqs 30 and 31,

$$D_0(Rh^+\text{−}L) = D_0(R\text{−}L) - E_0 \quad (30)$$

$$D_0(Rh\text{−}L) = D_0(R\text{−}L) - IE(Rh) + IE(R) - E_0 \quad (31)$$

where IE(Rh) = 7.459 eV,[42] IE(R) values are given in Table 2, and the D_0(R−L) values can be calculated from the thermochemistry given in Table 2.

(a) **RhH$^+$.** RhH^+ is observed in all three reaction systems, reactions 2, 8, and 20. We have previously determined

Table 3. Parameters of Eq 1 Used in Modeling the Reaction Cross Sections[a]

reaction		σ_0	n	E_0 (eV)
$Rh^+ + C_2H_6$	$\rightarrow RhH^+ + C_2H_5$	1.4(0.5)	1.8(0.1)	2.94(0.17)
	$\rightarrow C_2H_5^+ + RhH$	4.1(1.3)	1.5(0.1)	2.55(0.05)
	$\rightarrow RhCH_3^+ + CH_3$	1.3(0.2)	2.2(0.2)	2.34(0.06)
	$\rightarrow RhCH_2^+ + CH_4$	0.19(0.07)	2.1(0.2)	0.43(0.11)
	$\rightarrow RhC_2H_2^+ + 2H_2$	1.9(0.1)	0.8(0.1)	1.41(0.03)
$Rh^+ + C_3H_8$	$\rightarrow RhH^+ + C_3H_7$	0.44(0.07)	1.8(0.1)	3.00(0.12)
	$\rightarrow C_3H_7^+ + RhH$[b]	2.6(0.3)	2.3(0.1)	1.92(0.05)
		[1.1	2.1	1.69
		[3.2	2.1	2.47
	$\rightarrow RhC_3H_4^+ + 2H_2$	17.3(3.0)	1.1(0.3)	0.60(0.20)
	$\rightarrow RhC_2H_4^+ + CH_4$	0.71(0.16)	2.1(0.2)	0.21(0.10)
	$\rightarrow RhC_2H_2^+ + H_2 + CH_4$			0.6(0.2)[c]
	$\rightarrow RhCH_2^+ + C_2H_6$			0.5(0.2)
	$\rightarrow RhC_2H_5^+ + CH_3$	1.3(0.3)	1.3(0.4)	1.98(0.18)
	$\rightarrow RhCH_3^+ + C_2H_5$	0.87(0.19)	1.9(0.1)	2.46(0.10)
$Rh^+ +$ c-C_3H_6	$\rightarrow RhH^+ + C_3H_5$	0.78(0.26)	1.6(0.2)	3.16(0.19)
	$\rightarrow C_3H_5^+ + RhH$[b]	1.7(0.5)	2.3(0.2)	2.25(0.03)
		[0.2	2.1	1.65
		[3.5	1.7	2.85
	$\rightarrow RhCH_2^+ + C_2H_4$	10.4(2.5)	1.3(0.2)	0.21(0.05)
	$\rightarrow RhC_2H_4^+ + CH_2$			2.6(0.2)[c]
	$\rightarrow RhC^+ + H_2 + C_2H_4$	2.4(0.6)	1.6(0.3)	3.15(0.17)

[a] Uncertainties, in parentheses, are one standard deviation. [b] The description of these analyses is provided in the text. [c] Estimated value.

$D_0(Rh^+-H)$ in studies of the reactions of Rh^+ with H_2, HD, D_2, and CH_4.[17,19] The values obtained in these two studies, 1.67 ± 0.04 and 1.66 ± 0.05 eV, respectively, are in good agreement with each other and with theoretical values, Table 1. Thresholds for reactions 2, 8, and 20 calculated with this bond energy are lower than those measured here by about 0.3 eV, Table 3. This indicates that these reactions are suppressed at the thermodynamic thresholds by competition with the energetically more favorable reaction channels, formation of neutral RhH + R^+ (Figures 1, 3, and 4).

(b) RhH. Neutral rhodium hydride, RhH, is formed in reactions 3, 9, and 21. From the threshold measured for reaction 3, 2.55 ± 0.05 eV, $D_0(Rh-H)$ is calculated to be 2.42 ± 0.06 eV. For reactions 9 and 21, the values obtained for $D_0(Rh-H)$ depend on the structures of the R^+ ionic species formed. In previous studies of analogous reactions of Co^+, Ni^+, and Cu^+,[53,54] 2-$C_3H_7^+$ and c-$C_3H_5^+$ were believed to be formed, as these assumptions yielded consistent $D_0(M-H)$ values with those from C_2H_6 reactions. In the present study, the same assumptions lead to $D_0(Rh-H) = 2.19 \pm 0.06$ and 3.02 ± 0.04 eV from reactions 9 and 21, respectively. The alternative assumptions of 1-$C_3H_7^+$ and $CH_2CHCH_2^+$ structures lead to $D_0(Rh-H) = 2.97 \pm 0.06$ and 1.82 ± 0.10 eV, respectively. None of these values agrees particularly well with the value from reaction 3.

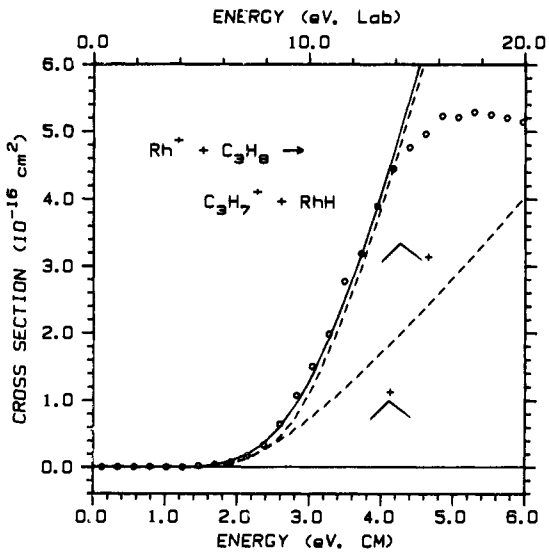

Figure 6. Cross section for $C_3H_7^+$ + RhH formed in the reaction of Rh^+ with C_3H_8 as a function of kinetic energy in the laboratory frame (upper axis) and center-of-mass frame (lower axis). The dashed lines indicate the two components, corresponding to two isomers of the $C_3H_7^+$ product, believed to comprise the experimental cross section, as detailed in the text. The full line is the sum of these two model components convoluted over the experimental kinetic energy distributions.

A plausible explanation for these disagreements is that *both* isomers are formed in reactions 9 and 21. To test this hypothesis, we attempted to model the cross sections for reactions 9 and 21 by including two parts corresponding to the formation of the two isomers. Each part is reproduced with eq 1 where E_0 is held at the value calculated for the corresponding isomer. Using $D_0(Rh-H) = 2.42 \pm 0.06$ eV measured from reaction 3, the thresholds for the formation of 2-$C_3H_7^+$ and 1-$C_3H_7^+$ in reaction 9 are calculated to be 1.69 ± 0.07 and 2.47 ± 0.07 eV, respectively; and for $CH_2CHCH_2^+$ and c-$C_3H_5^+$ in reaction 21 the thresholds are calculated to be 1.65 ± 0.11 and 2.85 ± 0.07 eV, respectively. The other parameters used in eq 1 are listed in Table 3. As shown in Figures 6 and 7, the cross

(42) Callender, C. L.; Hackett, P. A.; Rayner, D. M. *J. Opt. Soc. Am.* **1988**, *B5*, 614.
(43) Haynes, C. L.; Chen, Y.-M.; Armentrout, P. B. *J. Phys. Chem.* **1995**, *99*, 9110.
(44) Russo, N. In *Metal–Ligand Interactions: from Atoms, to Clusters, to Surfaces*; Salahub, D. R., Russo, N., Eds.; Kluwer Academic Publishers: The Netherlands, 1992; p 341.
(45) Moore, C. E. *Atomic Energy Levels*; Natl. Stand. Ref. Data Ser.; National Bureau of Standards: Washington, DC, 1971; Vol. II, NSRDS-NBS 35.
(46) Jacox, M. E. *J. Phys. Chem. Ref. Data* **1994**, Monograph 3.
(47) Aristov, N.; Armentrout, P. B. *J. Am. Chem. Soc.* **1984**, *106*, 4065.
(48) Carter, E. A.; Goddard, W. A., III *J. Phys. Chem.* **1988**, *92*, 2109.
(49) This value is based on ab initio calculations of: Pople, J. A.; Raghavachari, K.; Frisch, M. J.; Binkly, J. S.; Schleyer, P. v. R. *J. Am. Chem. Soc.* **1983**, *105*, 6389. Trinquier, G. *J. Am. Chem. Soc.* **1990**, *112*, 2130. This value agrees with a recent experimental determination of 3.2 ± 0.3 eV from ref 50.
(50) Schultz, R. H.; Armentrout, P. B. *Organometallics* **1992**, *11*, 828.
(51) Lias, S. G.; Bartmess, J. E.; Liebman, J. F.; Holmes, J. L.; Levin, R. D.; Mallard, W. G. *J. Phys. Chem. Ref. Data* **1988**, *17*, Supp. 1 (GIANT tables).
(52) Armentrout, P. B.; Beauchamp, J. L. *J. Am. Chem. Soc.* **1980**, *102*, 1736; **1981**, *103*, 784, 6628; *J. Chem. Phys.* **1981**, *74*, 2819.
(53) Georgiadis, R.; Fisher, E. R.; Armentrout, P. B. *J. Am. Chem. Soc.* **1989**, *111*, 4251.
(54) Fisher, E. R.; Armentrout, P. B. *J. Phys. Chem.* **1990**, *94*, 1674.

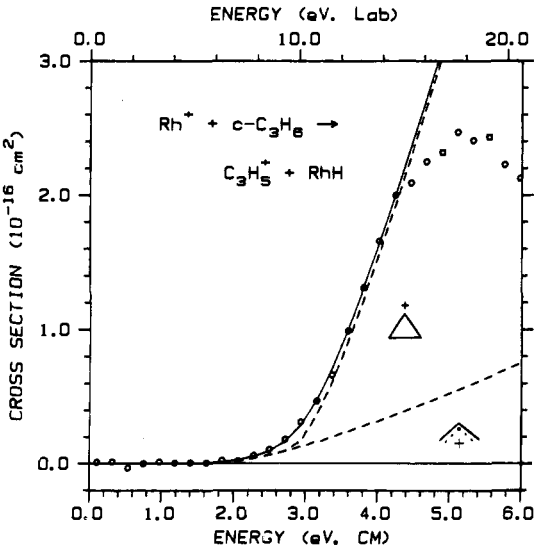

Figure 7. Cross section for $C_3H_5^+ + RhH$ formed in the reaction of Rh^+ with c-C_3H_6 as a function of kinetic energy in the laboratory frame (upper axis) and center-of-mass frame (lower axis). The dashed lines indicate the two components, corresponding to two isomers of the $C_3H_5^+$ product, believed to comprise the experimental cross section, as detailed in the text. The full line is the sum of these two model components convoluted over the experimental kinetic energy distributions.

sections for reactions 9 and 21 can be reproduced nicely by adding the two models, confirming the hypothesis. For reaction 9, the σ_0 parameters used in the two models have a ratio of 1:3, consistent with the ratio of the primary and secondary hydrogen atoms in the propane molecule. The n values used in the two models are the same, consistent with the chemical intuition that the formation of the two isomers should have similar energy dependences because both reactions correspond to simple C−H bond cleavages. For reaction 21, the model for formation of the higher energy c-$C_3H_5^+$ isomer has a smaller n value and a much larger σ_0 value than the model for the allyl $CH_2CHCH_2^+$ isomer, which means that the formation of c-$C_3H_5^+$ is a more efficient pathway relative to formation of $CH_2CHCH_2^+$. This is consistent with the fact that the former process involves only a simple C−H bond cleavage with retention of the cyclic structure, whereas the latter process involves both C−H and C−C bond cleavages.

On the basis of the analysis above, we take the value of 2.42 ± 0.06 eV from reaction 3 as our best measurement for D_0(Rh−H). The two values from reactions 9 and 21, which are based on the assumption of 2-$C_3H_7^+$ and c-$C_3H_5^+$ ionic product structures exclusively, are viewed as lower and upper limits for this bond dissociation energy. As can be seen from Table 1, our value agrees well with the previous ion beam study by Tolbert and Beauchamp,[18] in which D_0(Rh−H) was measured by bracketing the hydride affinity of Rh^+ in a study of the reactions of Rh^+ with a series of hydride donor reagents. However, our value is 0.35 ± 0.06 eV smaller than the theoretical value calculated by Langhoff, Pettersson, and Bauschlicher.[25,28]

From the cationic and neutral rhodium hydride BDE values, the ionization energy for RhH, IE(RhH), can be derived by using eq 32. This gives IE(RhH) = 8.21 ± 0.07 eV, which is larger

$$\mathrm{IE(RhH)} = D_0(\mathrm{Rh{-}H}) - D_0(\mathrm{Rh^+{-}H}) + \mathrm{IE(Rh)} \quad (32)$$

than the IE(R) values for R = C_2H_5, C_3H_7, and C_3H_5, Table 2. This is consistent with our observation that the $R^+ + RhH$ channel is energetically favored over $RhH^+ + R$ in all three reaction systems.

(c) $RhCH^+$ and RhC^+. In work on the reaction of Rh^+ with methane,[17] we have determined $D_0(Rh^+{-}CH)$ = 4.60 ± 0.12 eV and $D_0(Rh^+{-}C)$ = 4.38 ± 0.05 eV. The former value is in good agreement with 4.36 ± 0.3 eV obtained from photodissociation[21] (Table 1). The cross section data for RhC^+ formed in reaction 27 in the c-C_3H_6 system are analyzed using eq 1. The results give $D_0(Rh^+{-}C)$ = 4.12 ± 0.17 eV, in reasonable agreement with the value from the methane system. We take the average value of 4.25 ± 0.18 eV as our best measurement.

This value for $D_0(Rh^+{-}C)$ is much lower than the 7.1 ± 0.7 eV value obtained in a FTMS study[22] (Table 1), but that value is believed to be unreasonable. For example, for the first-row congener, $D_0(Co^+{-}C)$ = 3.6 ± 0.3 eV,[43] which is somewhat above $D_0(Co^+{-}CH_2)$ = 3.28 ± 0.05 eV[6a] and below $D_0(Co^+{-}CH)$ = 4.35 ± 0.38 eV.[43] Other first-row transition metals show similar relationships among the metal−carbide, −carbyne, and −carbene bond energies,[6a] indicating that the metal−carbide bond energy is essentially a double bond that can be augmented by back-donation of metal 4dπ electrons to the empty 2pπ orbital on the carbon atom. We note that our value for $D_0(Rh^+{-}C)$ has this relationship with $D_0(Rh^+{-}CH)$ and $D_0(Rh^+{-}CH_2)$ (Table 1), whereas the value obtained in the FTMS study is much larger than $D_0(Rh^+{-}CH)$.

(d) $RhCH_2^+$. Formation of $RhCH_2^+$ is observed in all three reaction systems via reactions 5, 16, and 26. By using eq 30 and the thresholds measured for reactions 5 and 26 (Table 3), $D_0(Rh^+{-}CH_2)$ = 3.61 ± 0.11 and 3.72 ± 0.06 eV are derived, respectively. Elsewhere, we obtain a value of 3.73 ± 0.07 eV from analysis of the reaction of Rh^+ with CH_4.[17] These three values are in excellent agreement within experimental error. A value for $D_0(Rh^+{-}CH_2)$ is not derived from results for reaction 16, because it is difficult to analyze the threshold definitively for the small tail shown in Figure 4. The apparent threshold of ~0.5 eV for this small tail yields $D_0(Rh^+{-}CH_2) \approx 3.67$ eV, consistent with the values obtained from the other reaction systems. The major feature in this $RhCH_2^+$ cross section cannot be assigned to alternative neutral products, such as $CH_3 + CH_3$, $CH_2 + CH_4$, or $H + C_2H_5$, because these channels lead to calculated thresholds higher than 4 eV.

We take the average of the three values, 3.69 ± 0.08 eV, as our best measurement for $D_0(Rh^+{-}CH_2)$. As can be seen from Table 1, this value is in good agreement with the photodissociation measurement by Hettich and Freiser,[21] 3.80 ± 0.22 eV, but lower than the value obtained using the bracketing technique by Jacobson and Freiser,[20] 4.01 ± 0.22 eV. The lower limit in this latter study of 3.79 eV (a 298 K value) was based on observing reaction 26 in their FTMS study and assuming that this observation indicated an exothermic reaction. The present study shows that this reaction is actually slightly endothermic, requiring that $D_0(Rh^+{-}CH_2) < 3.92$ eV (0 K value). Our value is also in good agreement with that calculated by Bauschlicher et al.,[31] but larger than those calculated by Musaev et al.[26,30] and Perry,[27] Table 1.

There are two questions regarding the $D_0(RhCH_2^+)$ value measured here that need discussion. The first is whether the $RhCH_2^+$ ion formed in the reactions studied is in its ground electronic state. Four independent calculations[27,30,31,44] indicate that $RhCH_2^+$ has a $^1A_1$ ground electronic state. Thus, the reactions forming $RhCH_2^+$ are all spin-forbidden processes, because the ground state of Rh^+ is ^3F[45] and all the neutral reactants and products involved have singlet ground states. Theoretical calculations by Musaev et al.[30] indicate that there are two nearly degenerate triplet excited states ($^3A_1$ and $^3A_2$) of $RhCH_2^+$ that lie about 0.2 eV higher than the ground state. The calculations by Perry[27] and Russo[44] indicate the triplet states

are 0.75 and 0.65 eV higher, respectively. It is conceivable that reactions 5 and 26 and the dehydrogenation of methane proceed along triplet potential energy surfaces to form excited triplet states of $RhCH_2^+$ in spin-allowed processes. This would mean that the $D_0(Rh^+-CH_2)$ values measured in these three systems would be 0.2 to 0.75 eV higher than the adiabatic BDE value. This appears not to be the case based on the good agreement between our BDE, the BDE calculated by Bauschlicher et al. for the singlet state,[31] and the BDE measured from the photodissociation study[21] (Table 1). Photodissociation of ground state $RhCH_2^+(^1A_1)$ to the $Rh^+(^3F) + CH_2(^3B_1)$[46] ground state asymptote is a spin-allowed process. Thus, reactions 5 and 26 and the dehydrogenation of methane appear to occur along adiabatic potential energy surfaces involving strong spin–orbit interactions, thereby allowing the formation of $RhCH_2^+$ in its singlet ground state. On the basis of those considerations, the $D_0(Rh^+-CH_2)$ value measured in this study is presumed to be the adiabatic BDE.

The second question about our measured $D_0(Rh^+-CH_2)$ value is whether the measured thresholds for reactions 5 and 26 and the dehydrogenation of methane correspond to their thermodynamic thresholds or activation barriers to these reactions. Theoretical calculations by Musaev et al.[30] indicate that there is an activation barrier to dehydrogenation of methane which lies 0.5 eV above the energy of the $RhCH_2^+ + H_2$ products. The excellent agreement among our measurements from the three systems suggests that no barriers exist, because the reaction mechanisms and the potential energy surfaces for these three reactions should be quite different, as discussed further below.

(e) $RhCH_3^+$. The $RhCH_3^+$ ion is formed in both alkane reaction systems (Figures 1–3) in reactions 4 and 17. From the thresholds measured for reactions 4 and 17 (Table 3), $D_0(Rh^+-CH_3)$ values are derived by using eq 30. This gives $D_0(Rh^+-CH_3) = 1.47 \pm 0.06$ and 1.32 ± 0.10 eV, respectively. The difference between these values is probably caused by the competition between reactions 17 and 18 in the C_3H_8 reaction system, processes that share the same intermediate, as discussed below. Because the $RhC_2H_5^+$ cross section is much larger than the $RhCH_3^+$ cross section in the threshold region (Figure 3c), reaction 17 might be suppressed at its threshold by reaction 18, and its apparent threshold shifted to slightly higher energies. This kind of competitive shift has been observed previously in the analogous reactions of Co^+, Ni^+, Cu^+,[53] and Ag^+ ion.[16] Thus, we take the value from reaction 17 as a lower limit for $D_0(Rh^+-CH_3)$, and the value of 1.47 ± 0.06 eV from reaction 4 as our best measurement for $D_0(Rh^+-CH_3)$.

As shown in Table 1, our measured value for $D_0(Rh^+-CH_3)$ is close to the theoretical values calculated by Bauschlicher et al.,[28] 1.61 eV, by Musaev and Morokuma, 1.63 eV,[26] and by Perry,[27] 1.65 eV, but 0.50 ± 0.23 eV smaller than the value obtained in a previous ion beam measurement by Mandich, Halle, and Beauchamp (MHB).[13] This study also obtained $D_0(Rh^+-CH_3)$ from the reaction of Rh^+ with ethane. As shown in Figure 2, the results are very similar, although a key difference occurs in the critical threshold region. The nonzero cross section below 2 eV measured by MHB is possibly due to the presence of excited states formed in the surface ionization source. The discrepancy between these experimental values is largely due to the details of the data analysis. Compared to our results, Table 3, Mandich et al. used a much higher value for the parameter n in eq 1 presumably because this was needed to reproduce the low-energy portion of the data. The quality of the present data and the lack of excited Rh^+ species allow a more definitive analysis of these data with less uncertainty.

In previous work, Jacobson and Freiser[20] concluded that the ground state structure of $RhCH_3^+$ was probably $H-Rh^+=CH_2$ rather than the rhodium–methyl cation. This conclusion was based on the bond energy for $RhCH_3^+ \rightarrow RhCH_2^+ + H$, 2.7 ± 0.4 eV, which was taken from the thermochemistry measured previously. We find a similar bond strength of 2.49 ± 0.10 eV based on the present thermochemistry. Jacobson and Freiser noted that this value is substantially less than the BDE of a typical C–H bond, and much closer to that for Rh^+-H. This simple comparison fails to consider that $RhCH_2^+$ has a $^1A_1$ ground state,[27,30,31,44] and thus has no unpaired electrons to form a covalent bond with H. The $HRhCH_2^+$ species could be formed by coupling to a triplet excited state of $RhCH_2^+$, calculated to lie 0.2 to 0.75 eV above the ground state.[27,30,44] The exchange energy lost upon bonding H to one of these triplet $RhCH_2^+$ species is probably comparable to that for Rh^+, also a triplet, such that the $H-Rh^+$ bond strength should be stronger than that for $H-RhCH_2^+$ by the $RhCH_2^+$ triplet excitation energy in the latter case. This would place the adiabatic $H-RhCH_2^+$ bond energy at 0.9 to 1.5 eV, much weaker than the experimental 2.49 ± 0.10 eV value. Therefore, in contrast with Jacobson and Freiser, we conclude that $RhCH_3^+$ has the methyl structure, as also suggested by the reasonable agreement between the theoretically calculated Rh^+-CH_3 bond energy and that measured here, Table 1. The $RhCH_2^+-H$ bond strength is weaker than a typical C–H bond because it is stabilized by the formation of a strong $Rh-CH_2$ π bond. Hettich and Freiser also point out this latter possibility.[21]

(f) $RhC_2H_5^+$. This ion is formed in the C_3H_8 reaction system in reaction 18. When the E_0 measured for this reaction (Table 3) is combined with $D_0(C_2H_5-CH_3)$, we find $D_0(Rh^+-C_2H_5) = 1.80 \pm 0.18$ eV. The structure of the $RhC_2H_5^+$ species could be either a rhodium–ethyl cation or a hydrido–rhodium–ethene ion complex, $HRh^+(C_2H_4)$. If the structure is the former, the rhodium–ethyl bond energy is 0.33 ± 0.19 eV stronger than the rhodium–methyl bond energy. Results for six first-row transition-metal ions indicate that $D_0(M^+-C_2H_5)$ are an average of 0.12 ± 0.20 eV stronger than $D_0(M^+-CH_3)$,[6a] and Perry[27] has calculated that $D_0(Rh^+-C_2H_5)$ is 0.33 eV stronger than $D_0(Rh^+-CH_3)$. These results strongly implicate the rhodium–ethyl structure as our ground state structure. However, if we consider the alternative structure, for which calculations were not explicitly performed, the thermochemistry measured here gives $D_0[HRh^+-C_2H_4] = 1.63 \pm 0.18$ eV, comparable to $D_0(Rh^+-C_2H_4) > 1.34$ eV determined below and to $D_0(Rh^+-C_2H_4) = 1.78$ eV calculated by Perry.[27] Thus, the hydrido–rhodium–ethene ion structure is also reasonable. Although a definitive structure determination cannot be made, it seems likely that $RhC_2H_5^+$ has the rhodium–ethyl ion structure, a conclusion based largely on the strength of the comparison with theory.

(g) Bond-Energy Bond-Order Correlation for Rh^+-CH_x Bonds. One interesting way of investigating the bond order of simple metal ligand species is to compare with organic analogues, i.e. $D_0(Rh^+-L)$ vs $D_0(L-L)$.[47] Such a plot is shown in Figure 8, and differs somewhat from a previous version.[21] It can be seen that the correlation is remarkably good which indicates that Rh^+-H, Rh^+-CH_3, and plausibly $Rh^+-C_2H_5$ are all single bonds, $Rh^+=CH_2$ is a double bond, and $Rh^+\equiv CH$ is a triple bond. The bonding character of Rh^+-O is discussed in detail elsewhere,[34] but it is predicted to have a bond order of 2.[48] A reasonable correlation is therefore found when we plot the RhO^+ BDE vs $D_0(O=O) = 5.12$ eV and $D_0(H_2C=O) = 7.66$ eV. These two molecules both have a bond order of two but different numbers of antibonding electrons. The point that lies furthest from the line is for Rh^+-C, correlated with the

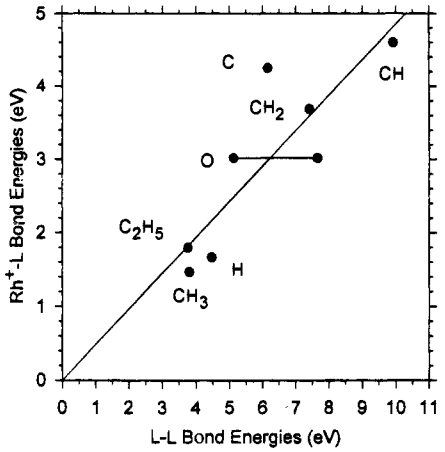

Figure 8. Correlation of Rh^+-L bond energies with those for the organic analogues, L−L, except in the case of O where the bond energies of O_2 and H_2CO are used as references. Values are from Table 1 and information in Table 2.

bond energy of C_2. In this case, the RhC^+ bond energy lies above the line because the covalent double bond in this molecule can be augmented by back donation of a doubly occupied $4d\pi$ orbital on Rh^+ into the empty $2p\pi$ orbital on C, something that C_2 cannot do.

(h) $RhC_2H_4^+$. This ion is formed in the C_2H_6, C_3H_8, and c-C_3H_6 systems in reactions 6, 14, and 28. Reaction 6 is exothermic (Figure 3), establishing that $D_0(Rh^+-C_2H_4) > 1.34$ eV. Deuterium isotope labeling studies of Tolbert et al. indicate that this reaction occurs by 1,2-elimination,[12] indicating a Rh^+(ethene) structure. This lower limit is consistent with $D_0(Rh^+-C_2H_4) = 1.32 \pm 0.2$ eV, a value derived from the estimated threshold for reaction 28, 2.6 ± 0.2 eV (Table 3). We hesitate to assign this value to this bond energy because of the severe competition between reaction 28 and the much more efficient process 26. Indeed, Perry[27] has calculated that $D_0(Rh^+-C_2H_4) = 1.78$ eV, and his value for $Co^+-C_2H_4$ of 1.95 eV is in good agreement with our experimental value of 1.86 ± 0.07 eV.[6a]

This lower limit also indicates that reaction 14 is exothermic by >0.54 eV, but as shown in Figure 3b, the cross section for this reaction exhibits endothermic behavior. Thus, the measured threshold of 0.21 ± 0.10 eV (Table 3) is believed to represent an activation barrier to this methane elimination channel, as discussed further below. Another possibility is the formation of the ethylidene isomer, $Rh^+{=}CHCH_3$, in which case the threshold indicates that $D_0(Rh^+-CHCH_3) = 3.36 \pm 0.11$ eV. This bond energy is somewhat smaller than $D_0(Rh^+-CH_2) = 3.69 \pm 0.08$ eV measured here, but the discrepancy is not sufficient to definitively rule out this possibility.

(i) $RhC_2H_2^+$. This ion is formed in the C_2H_6, C_3H_8, and c-C_3H_6 systems in reactions 7, 15, and 25, respectively. Reaction 7 is a double dehydrogenation channel. The threshold measured for this reaction, 1.41 ± 0.03 eV (Table 3), gives a value of $D_0(Rh^+-C_2H_2) = 1.67 \pm 0.03$ eV. This is considerably stronger than the value calculated by Sodupe and Bauschlicher, 1.27 eV.[33] One possible explanation is that we form the $Rh^+{=}CCH_2$ structure, in which the case the threshold yields $D_0(Rh^+{=}CCH_2) = 3.73 \pm 0.17$ eV, very similar to $D_0(Rh^+{=}CH_2)$, Table 1. On the basis of this thermochemistry, the structure of $RhC_2H_2^+$ cannot be determined unambiguously.

Using the thermochemistry determined from reaction 7, we calculate that reaction 25 should be exothermic by 0.72 ± 0.03 eV (even if the weaker theoretical $Rh^+-C_2H_2$ bond energy is used in this calculation, the reaction is still exothermic); however, Figure 5b shows that the cross section for this reaction increases slightly with increasing energy, usually a mark of an endothermic process. Other possible assignments of the neutral products (e.g., CH_3 + H and H_2 + CH_2) lead to calculated thresholds higher than 3.7 eV, which are inconsistent with the data (Figure 5b). Thus, reaction 25 appears to be hindered by competition with reaction 23, which must be much more facile kinetically.

For reaction 15, we calculate that the threshold should be 0.87 ± 0.03 eV. This is close to the threshold estimated for the low-energy feature of reaction 15, 0.6 ± 0.2 eV. It is possible that the two features observed in this cross section correspond to the $Rh^+{=}CCH_2$ and Rh^+(ethyne) structures, and the comparison with theoretical thermochemistry would suggest that the higher energy feature would correspond to the latter structure.

(j) $RhC_3H_4^+$ and $RhC_3H_6^+$. Formation of $RhC_3H_4^+$ in the C_3H_8 reaction system is a double dehydrogenation process, reaction 13. The threshold measured for this reaction, 0.60 ± 0.20 eV, gives $D_0(Rh^+-C_3H_4) = 2.3 \pm 0.2$ eV. This is larger than the $D_0(Rh^+-C_2H_2)$ of 1.67 ± 0.03 eV, which might be evidence that the $Rh^+(CH_2{=}C{=}CH_2)$ isomer rather than the Rh^+(propyne) isomer is formed. Isomers such as $Rh^+{=}CHCH{=}CH_2$ might also be considered. Taking $\Delta_fH(CHCH{=}CH_2)$ as 4.5 ± 0.2 eV [based on adding $\Delta_fH(CH_3CH{=}CH_2)$ to the difference between $\Delta_fH(CHCH_3)$ = 3.4 ± 0.1 eV[49,50] and $\Delta_fH(C_2H_6)$, Table 2], we find that the measured threshold corresponds to $D_0(Rh^+{=}CHCHCH_2) = 4.7_5$ ± 0.3 eV. Although stronger than $D_0(Rh^+{=}CH_2)$, this bond strength could be augmented by the interaction between Rh^+ and the C−C π bond.

Formation of $RhC_3H_4^+$ in the c-C_3H_6 system is an exothermic dehydrogenation process (Figure 5a). We discount the possibility that this is cyclopropene bound to Rh^+ because dehydrogenation of cyclopropane costs 2.3 eV,[51] and the bond energy of Rh^+ to cyclopropene is unlikely to exceed this energy. In contrast, dehydrogenation of cyclopropane to form allene or propyne costs only 1.34 and 1.27 eV, respectively (Table 2), and formation of $CHCH{=}CH_2$ is estimated (as outlined above) to require 3.8 ± 0.2 eV. Given the thermochemistry derived above, formation of Rh^+ bound to these species should be exothermic, consistent with experiment and making it impossible to ascertain what structure the $RhC_3H_4^+$ product adopts. Alternatively, one could retain the cyclic structure to form $Rh^+{=}\overline{CCH_2CH_2}$, a molecule for which it is difficult to reliably estimate the thermodynamics.

The exothermic reaction 12 in the C_3H_8 system sets a lower limit of $D_0(Rh^+-C_3H_6) > 1.22$ eV.

Reaction Mechanisms. In the previous studies,[10,12] the activation of small alkanes by Rh^+ has been explained by an oxidative addition mechanism. In such a mechanism, Rh^+ inserts into a C−H or C−C bond to form $R-Rh^+-H$ and $R'-Rh^+-CH_3$ intermediates. Products can be formed by reductive elimination of small molecules such as H_2 and CH_4 through rearrangement of the intermediate by β-H or β-CH_3 transfers at low energies, and by metal−hydrogen or metal−carbon bond cleavage at high energies. This mechanism is also invoked to interpret experimental observations for the reactions of the first-row congener, Co^+, with alkanes.[52-54]

Recent theoretical work calls this time-honored mechanism into question for reactions of Rh^+ with alkanes. Blomberg et al.[15] estimate that the barrier for insertion of Rh^+ into the C−H bond of ethane should "fall very close to or below the ground-state dissociation limit", suggesting that this mechanism is a viable one. Perry,[27] on the other hand, estimates that the

Scheme 1

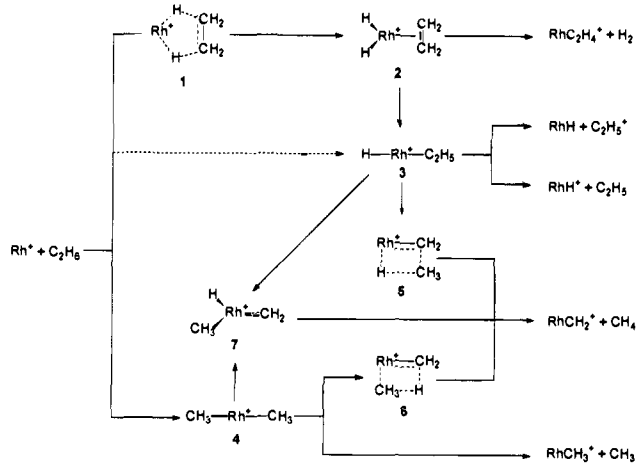

$H-Rh^+-C_2H_5$ intermediate, which is a ground state singlet, lies 0.30 ± 0.22 eV higher than the $Rh^+ + C_2H_6$ reactants (the triplet state of this intermediate lies 0.39 ± 0.17 eV above the reactants). Perry concludes that the standard mechanism cannot explain the *exothermic, barrierless* dehydrogenation of C_2H_6 by Rh^+, although it is the lowest energy pathway for Co^+ (which experimentally[53] and theoretically[27] is observed to have a barrier). He then calculates that there is an alternative mechanism for this process that has no barriers in excess of the reactants' energy. This involves a concerted insertion of Rh^+ into C−H bonds on adjacent carbons to directly form the $H_2Rh(C_2H_4)^+$ intermediate, which then reductively eliminates H_2. The standard mechanism is capable of explaining our experimental observations (apart from the question of the relative energetics of all intermediates), but the alternative mechanism of Perry offers much in explaining the differences between the reactivities of Rh^+ and Co^+. Therefore, in the following, we assume that Perry's mechanism for dehydrogenation of ethane is correct and explore its implications for the other reaction channels observed and for the other systems studied.

(a) C_2H_6. Scheme 1 shows the mechanism for reaction of Rh^+ with C_2H_6. At the lowest kinetic energies, Rh^+ can simultaneously insert into two C−H bonds via transition state **1** in which the transferring H atoms lie above the Rh−C−C plane. This forms intermediate **2**, which is calculated to have a singlet ground state and where the H−Rh−H plane is perpendicular to the Rh−C−C plane. **2** can then reductively eliminate H_2 to form $RhC_2H_4^+ + H_2$, where the rhodium−ethene cation is calculated to have a triplet ground state. Thus, the overall process involves two spin changes (triplet−singlet−triplet) but is calculated to have no barriers in excess of the energy of the reactants, consistent with experimental observation, Figure 1. At higher energies, we observe reactions 2 and 3 in which ethyl radicals and ions are formed. These processes presumably occur via intermediate **3**, $H-Rh^+-C_2H_5$, which could be formed either by a H-atom transfer from **2** (the reverse of the mechanism usually proposed) or by direct insertion of Rh^+ into the C−H bond of ethane. Although **3** is calculated by Perry[27] to lie 0.30 ± 0.22 eV above the reactants (and hence is probably not involved in the exothermic dehydrogenation reaction), this is below the energy of the product channels for reactions 2 and 3. Therefore, direct insertion is a likely pathway for these reactions which can both take place along a triplet surface (given that **3**[55] and RhH[56] have triplet ground states and RhH^+ has a doublet ground state[23,24,26,27]).

(55) Perry (ref 27) calculates that $H-Rh^+-CH_3$ has a triplet ground state.
(56) Langhoff, S. R.; Pettersson, L. G. M.; Bauschlicher, C. W., Jr.; Partridge, H. *J. Chem. Phys.* **1987**, *86*, 268.

In the Results section, we noted that reactions involving C−H bond cleavage, such as reactions 3 and 6, have much larger cross sections than those for C−C bond cleavage, reaction 4 (Figure 1). Formation of $RhCH_3^+ + CH_3$ presumably occurs via the C−C bond insertion intermediate **4**, calculated by Perry to lie 0.13 eV above the reactants and 0.17 eV below intermediate **3**, the C−H bond insertion intermediate. Because formation of $RhCH_3^+ + CH_3$ from intermediate **4** is a simple Rh−C bond cleavage process, it is unlikely to have a reverse activation barrier in its exit channel. Thus, the reactivity difference between C−H and C−C cleavage processes must be caused by differences in the entrance channel, and suggests that C−C bond activation is more constrained. This is consistent with calculations,[57,58] which indicate that at the transition state for C−C insertion, the two methyl groups have to tilt toward the Rh^+ to make reasonable Rh−C bonds but this weakens the C−C bond. In contrast, C−H bond activation reactions can occur via the low-energy pathway of Perry or by direct C−H bond insertion at higher kinetic energies. In both mechanisms, the spherical H atom can bind both the Rh^+ and carbon atom simultaneously. These conclusions are in direct accord with those made by Jacobson and Freiser based on the thermal reactivity of $RhCD_2^+$ with CH_4.[20]

There are two plausible pathways to form $RhCH_2^+ + CH_4$, reaction 5, from $Rh^+ + C_2H_6$, as shown in Scheme 1: (a) intermediate **3** rearranges to form the four-centered transition state, structure **5**; (b) intermediate **4** forms the four-centered transition state, structure **6**. The first two pathways were originally suggested by Jacobson and Freiser, who obseved that $RhCH_2^+$ reacts with CH_4 to form $Rh^+ + C_2H_6$ and $RhC_2H_4^+ + H_2$ at thermal energies.[20] This observation indicates that the pathway involving **5** is certainly lower in energy than $RhCH_2^+ + CH_4$. This is consistent with the 0.43 ± 0.11 eV thermodynamic threshold measured for $RhCH_2^+$ production here. Further, these observations imply that the energies of structures **2**−**6** lie below this threshold, consistent with the calculations of Perry.[27] The plausibility of these pathways is partly based on the calculations of Musaev, Koga, and Morokuma, who found a four-centered transition state for dehydrogenation of methane by Rh^+ to form $RhCH_2^+$.[30] Unpublished work by Perry[59] suggests that this reaction might proceed by formation of a stable $(H)_2RhCH_2^+$ intermediate instead. On the basis of this work, rearrangement of **4** by an α-H shift or of **3** by an α-CH_3 shift to form intermediate **7** which would then reductively eliminate methane could also be viable mechanisms for reaction 5 and its reverse.

(b) C_3H_8. Much of the mechanism for reaction of Rh^+ with propane should be directly analogous to that for ethane. The concerted insertion of Rh^+ into C−H bonds on adjacent carbons to form a dihydrido−rhodium−propene intermediate analogous to **2** followed by the reductive elimination of H_2 provides the mechanism for the dominant dehydrogenation process 12. The exothermic behavior of this reaction indicates that there is no activation barrier along this path that is higher in energy than the $Rh^+ + C_3H_8$ reactants. Subsequent dehydrogenation of the $RhC_3H_6^+$ product ion yields $RhC_3H_4^+$. At higher energies, rearrangement of this intermediate or direct C−H insertion to form $H-Rh^+-C_3H_7$ (analogous to **3**) provides a pathway for the dominant high-energy processes 8, 9, and 10.

A more interesting question concerns the mechanism by which a C−C bond is activated. The lowest energy reaction

(57) Low, J. J.; Goddard, W. A., III *J. Am. Chem. Soc.* **1984**, *106*, 6928, 8321; **1986**, *108*, 6115; *Organometallics* **1986**, *5*, 609.
(58) See: Siegbahn, P. E. M.; Blomberg, M. R. A. *J. Am. Chem. Soc.* **1992**, *114*, 10548 and references therein.
(59) Perry, J. K. Personal communication.

Scheme 2

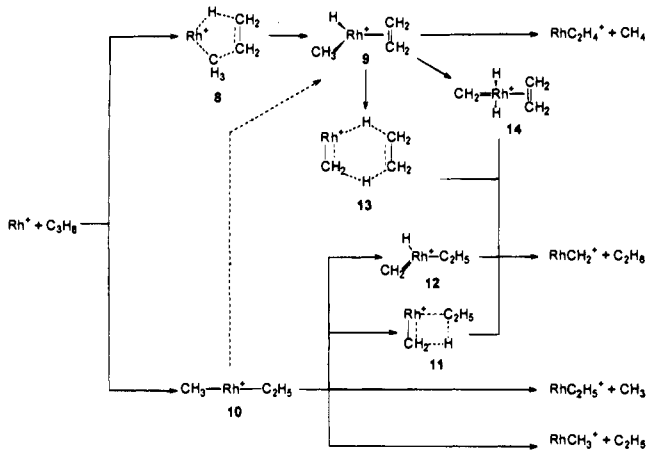

Scheme 3

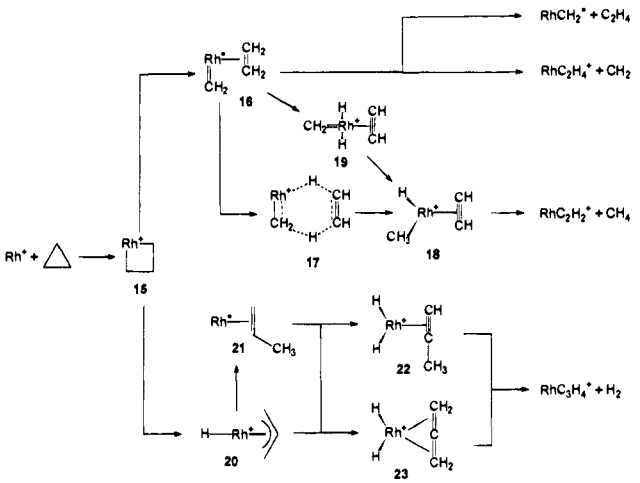

of this type is formation of $RhC_2H_4^+ + CH_4$, an overall exothermic process that clearly exhibits a barrier, Figure 3b, which we measure as 0.21 ± 0.10 eV. One possible pathway is a concerted process analogous to that calculated by Perry, that is, generation of the transition state **8** to directly form intermediate **9**, Scheme 2. As one of the groups transferring from the incipient ethene ligand to rhodium is now a methyl group rather than a hydrogen atom, the sp^3 directionality of the methyl orbital could result in the barrier observed. We should also consider the conventional mechanisms in which intermediate **9** is formed either by Rh^+ insertion into the primary C−H bond to form $H-Rh^+-C_3H_7$ followed by transfer of a β-CH_3 group, or by Rh^+ insertion into the C−C bond to form intermediate **10** followed by β-H transfer. As noted above, Perry calculates that the C−H insertion process is endothermic by 0.30 ± 0.22 eV for the case of ethane with only a small barrier in excess of this endothermicity. Insertion into a primary C−H bond of propane should exhibit comparable thermochemistry, such that this would explain the barrier observed for reaction 14. Regarding the C−C insertion process, Perry estimates that $Rh(CH_3)_2^+$ lies 0.13 eV higher in energy than $Rh^+ + C_2H_6$. He further calculates that the $HRh^+-C_2H_5$ bond strength is larger than that for the HRh^+-CH_3 bond by 0.21 eV. If we assume that $D_0(H_3CRh^+-C_2H_5)$ exceeds $D_0(H_3CRh^+-CH_3)$ by a comparable amount, then **10** lies slightly below the energy of the reactants. The barrier associated with the C−C bond insertion could then explain our observations for reaction 14.

Further insight into this mechanism comes from FTICR studies of the reaction of $RhCH_2^+$ with C_2H_6.[20] There it was observed that the reaction rapidly forms $RhC_2H_4^+ + CH_4$ (92%) and $Rh^+ + C_3H_8$ (8%), but no $RhC_3H_6^+ + H_2$, even though the latter is more exothermic than the $Rh^+ + C_3H_8$ channel. The mechanism of this reaction (and therefore of reaction 16, too) is not obvious, but must avoid formation of the $H_2Rh(C_3H_6)^+$ intermediate that leads to dehydrogenation. One possibility (suggested by Jacobson and Freiser) is addition of a C−H bond across the $Rh^+=CH_2$ π bond to form the four-centered intermediate **11** (analogous to **6**) which then forms intermediate **10**. Another possibility is oxidative addition of a C−H bond to the Rh center to form intermediate **12**, which then rearranges to **10**. Other intriguing possibilities are concerted processes in which two C−H bonds adjacent carbons of ethane add to $RhCH_2^+$. If this addition occurs across the $Rh^+=CH_2$ π bond, this yields the six-centered transition state **13** that leads directly to intermediate **9** and has orbital character similar to a 4 + 2 cycloaddition. Concerted addition to the Rh center leads to intermediate **14**, which can rearrange to **9** by a H transfer. As discussed in the results section, reaction 16 occurs at its thermodynamic threshold but is inefficient, and at higher energies, the reaction increases in probability. If the low-energy pathway corresponds to one of the concerted and sterically demanding intermediates, then the inefficiency could be explained by suppression of reaction 16 by the kinetically and thermodynamically more favorable formation of $RhC_2H_4^+ + CH_4$. The high-energy feature could then be attributed to the pathways involving **11** or **12**. Note that the FTICR results indicate that elimination of propane from the reaction intermediate is more constrained than elimination of methane. This observation suggests either that the **13**−**9** or **14**−**9** pathways are preferred or that the rearrangement of **10** to **9** is facile compared to propane elimination.

(c) c-C_3H_6. Scheme 3 shows some of the reaction mechanism for the reaction of Rh^+ with c-C_3H_6. It is generally accepted[54,60,61] that C−C bond activation of c-C_3H_6 by metal ions initially leads to formation of the metallacyclobutane ion, intermediate **15**. Cleavage across the metallacycle yields intermediate **16**, which can lose C_2H_4, reaction 26, or CH_2, reaction 28. A speculative rearrangement of **16** to form intermediate **18**, which can reductively eliminate methane, is a concerted addition of adjacent C−H bonds on the ethene ligand to the $RhCH_2^+$. If this occurs across the $Rh^+=CH_2$ π bond, transition state **17**, then **18** is formed directly. Alternatively, addition can occur to the Rh center, in which case intermediate **19** is formed and **18** is produced by α-H transfer. In either case, reactions 25 and 26 share common intermediates explaining why the cross section for the low-energy, but kinetically difficult methane elimination reaction declines once the facile ethene elimination reaction becomes energetically available, Figure 5b. An alternative path for reaction 25 that involves more conventional transition states has been previously outlined for the Co^+ system.[54]

Intermediate **15** can also rearrange by β-H migration to intermediate **20**, which can cleave the Rh−allyl bond to form $RhH^+ + CH_2CHCH_2$ and $RhH + CH_2CHCH_2^+$. Alternatively, products with these masses can be formed by initial C−H insertion leading to a hydridocyclopropylrhodium cation which can dissociate by Rh−C bond cleavage to yield $RhH^+ +$ c-C_3H_5 and $RhH +$ c-$C_3H_5^+$. Intermediate **20** can also rearrange to intermediate **21**, Rh^+−propene, which could eliminate propene in an exothermic reaction that cannot be monitored in our

(60) Armentrout, P. B.; Beauchamp, J. L. *J. Chem. Phys.* **1981**, *74*, 2819. Georgiadis, R.; Armentrout, P. B. *Int. J. Mass Spectrom. Ion Processes* **1989**, *89*, 227.

(61) Sunderlin, L. S.; Armentrout, P. B. *J. Phys. Chem.* **1990**, *94*, 3589.

experimental study because the reactant and product ions are the same. The structure of the $RhC_3H_4^+$ ion formed by dehydrogenation is unclear. The cyclic structure $Rh^+{=}\overline{CCH_2CH_2}$ can be formed by α-hydrogen elimination from the hydridocyclopropyl intermediate. Scheme 3 shows that formation of Rh^+−propyne and Rh^+−allene can proceed through additional H migrations from intermediates **20** and **21** to form intermediates **22** and **23**, respectively, which can reductively eliminate H_2. Alternatively, a concerted addition of two adjacent C−H bonds in **21** could also form **22** and **23**. Another possibility is formation of $Rh^+{=}CHCH{=}CH_2$ which could occur by α-H migration from intermediate **20**. The observation that dehydrogenation occurs with no activation barrier higher than the energy of the Rh^+ + c-C_3H_6 reactants demonstrates that there is a high level of hydrogen mobility. Even more uncertain is the structure of the $RhC_3H_2^+$ ion, but species involving carbides may be reasonable possibilities here.

Reactivity Differences between Rh^+ and Co^+. The reactions of Co^+ (the first-row congener of Rh^+) with C_2H_6, C_3H_8, and c-C_3H_6 have been studied previously.[52-54,62] The differences in reaction behavior between Rh^+ and Co^+ reactions can be summarized fairly succinctly. First, formation of MCH_2^+ + RH in reactions 5 and 16 and dehydrogenation of methane (R = CH_3, C_2H_5, and H, respectively), which involve four-centered transition states (except possibly in the propane system, see Scheme 2), occurs at their thermodynamic thresholds in the Rh^+ systems, whereas the corresponding reactions in the Co^+ systems exhibit activation barriers and are relatively inefficient. Second, exothermic dehydrogenation processes, reactions 6, 12, and 23, are observed to be exothermic and efficient in the Rh^+ systems, whereas the corresponding reactions in the Co^+ systems are relatively inefficient. In the C_3H_8 system, the comparable dehydrogenation reaction is an order of magnitude smaller for Co^+; in the C_2H_6 system, an activation barrier to this exothermic process is observed; and the reaction is not observed at all in the cyclopropane system.[53,54] Third, elimination of methane in the Rh^+ + C_3H_8 system, reaction 14, encounters an activation barrier, whereas the corresponding reaction in the Co^+ + C_3H_8 system is observed to be exothermic and relatively efficient (about three times less efficient at thermal energies than dehydrogenation).[53,65]

The observation that the energies of four-centered transition states in the Co^+ reaction systems are higher than those in the Rh^+ systems is consistent with the relative barriers determined in theoretical calculations by Musaev et al. for the reactions of $MCH_2^+ + H_2 \rightarrow M^+ + CH_4$. For Co^+, they calculate a barrier about 1.1 eV above the reactants,[63] compared with a 0.5 eV barrier for the Rh^+ system.[30] As noted above, the present experimental results disagree with the magnitude of the barrier for the Rh^+ system. Likewise we have measured a lower barrier for the Co^+ system,[43] but the relative size of the barriers is consistent with theory. The way to understand this difference is to consider simple molecular orbital ideas that parallel our discussion of the activation of H_2 and CH_4 by metal oxide ions.[64] As discussed in detail elsewhere,[2,3] activation of covalent bonds at transition-metal centers is most facile when the metal has an empty s-like valence orbital to accept the pair of electrons in the covalent bond, and when it has a pair of valence dπ-like electrons to donate into the antibonding orbital of the bond to be broken. For the metal methylidenes, the valence molecular orbitals (MOs) are the following: $1a_1$ and $1b_1$ M−C bonding; $1a_2$, $1b_2$, and $2a_1$ d-like nonbonding; a $3a_1$ s-like nonbonding; and $2b_1$ and $4a_1$ antibonding. For these species, the most likely acceptor orbital is the $3a_1$ s-like MO and the donor orbital is one of the nonbonding d-like orbitals. $CoCH_2^+$ has a $^3A_2$ ground state with a $(1a_1)^2(1b_1)^2(1a_2)^1(1b_2)^2(2a_1)^2(3a_1)^1$ electron configuration, while $RhCH_2^+$ has a $^1A_1$ ground state with a $(1a_1)^2(1b_1)^2(1a_2)^2(1b_2)^2(2a_1)^2(3a_1)^0$ electron configuration. This difference in ground state configurations can be attributed to the higher energy of the s orbital in the Rh^+ system compared with the first-row metals. Thus, both systems have doubly occupied d-like donor orbitals, but the $3a_1$ acceptor orbital is occupied in the $CoCH_2^+$ system, thereby leading to a more repulsive interaction and an activation barrier. The acceptor orbital is empty in the $RhCH_2^+$ system, thereby avoiding the repulsive interactions. The comparable $^1A_1$ state for $CoCH_2^+$ is calculated to be fairly high in energy (1.1 eV above the ground state)[30] and therefore not a viable path for reaction.

Previous work has indicated that the rate limiting step in the dehydrogenation of propane by Co^+ occurs when the C−H bond oxidatively adds to the Co^+ center.[65] While this transition state lies below the energy of the reactants in the propane system, it is higher in the ethane system because the interaction of Co^+ with ethane at long range is weaker than with propane due to the relative polarizabilities of the two alkanes. According to Perry,[27] oxidative addition of C−H bonds to Rh^+ should be less facile than to Co^+, because the energy of the comparable transition state is higher for the second-row metal ion. Thus, Perry's calculations indicate that the efficient dehydrogenation of alkanes by Rh^+ is driven by the stability of the H_2M^+(alkene) intermediate which can be formed by the concerted process discussed above. For the ethane case, this species is calculated to be a singlet and estimated to be bound (relative to M^+ + C_2H_6) by 0.87 eV when M = Rh. In contrast, when M = Co, the intermediate is a ground state triplet that does not appear to be a minimum on the potential energy surface and is unbound by 0.69 eV (the singlet state lies 0.30 eV higher). Thus, Perry[27] proposes that dehydrogenation of alkanes by Co^+ forms H−Co^+−alkyl which then eliminates H_2 in a multicenter process, rather than by forming H_2Co^+(alkene).

Previous work has indicated that methane elimination from propane as induced by Co^+ at thermal energy proceeds by primary C−H bond activation to form H−Rh^+−*n*-C_3H_7 followed by β-methyl transfer and methane elimination with the first step being rate limiting, as noted above.[65] At higher energies, a second pathway for methane elimination is believed to become important, namely, initial C−C bond insertion to form an intermediate analogous to **10**, followed by β-H migration and methane elimination.[53,65] This path accounts for the observation that methane elimination is more favorable than dihydrogen elimination at energies above 1 eV. The failure to observe methane elimination at thermal energies in the Rh^+ system appears to be because the C−H bond activation process, low energy in the Co^+ system, has a barrier for Rh^+. The reductive elimination step is not rate limiting in the Rh system because, as noted previously,[10,12] the reverse of this step, addition of methane to Rh(alkene)$^+$ species, is more efficient than that to Co(alkene)$^+$ species.

Overall, Perry[27] attributes the differences in the reaction behavior of Co^+ vs Rh^+ to be because the s^1d^7 configuration is more accessible for Co^+ and sd hybridization is more effective for Rh^+. (The excitation energy of the $^5F(5s^14d^7)$ state of Rh^+ is 2.1 eV, while the comparable state for Co^+ lies at 0.42 eV.)

(62) Haynes, C. L.; Armentrout, P. B. *Organometallics* **1994**, *13*, 3480.
(63) Musaev, D. G.; Morokuma, K.; Koga, N.; Nguyen, K. A.; Gordon, M. S.; Cundari, T. R. *J. Phys. Chem.* **1993**, *97*, 11435.
(64) Clemmer, D. E.; Aristov, N.; Armentrout, P. B. *J. Phys. Chem.* **1993**, *97*, 544.
(65) van Koppen, P. A. M.; Brodbelt-Lustig, J.; Bowers, M. T.; Dearden, D. V.; Beauchamp, J. L.; Fisher, E. R.; Armentrout, P. B. *J. Am. Chem. Soc.* **1991**, *113*, 2359.

The former effect stabilizes intermediates like $H-M^+-$alkyl while the latter stabilizes intermediates like H_2M^+(alkene). The relative stabilities of these intermediates then controls the reaction pathways available to the two metals.

Conclusion

Ground state Rh^+ ions are found to be very reactive with C_2H_6, C_3H_8, and c-C_3H_6 over a wide range of kinetic energies. Efficient dehydrogenation is observed at thermal energies in all three reaction systems. At high energies, the dominant process in the ethane and propane systems is C−H bond cleavage to form RhH + R^+ (where R = ethyl and propyl, respectively). In contrast, the cyclopropane system is dominated by C−C bond cleavage to form $RhCH_2^+ + C_2H_4$ at elevated energies. The endothermic reaction cross sections are modeled to yield 0 K bond dissociation energies for several Rh−ligand species as summarized in Table 1. In most cases, reasonable agreement is found for these values compared with previous experimental and theoretical work, although ambiguities exist in the structures of several $RhC_xH_y^+$ species where $x \geq 2$.

Possible reaction mechanisms for the reactions of Rh^+ with these hydrocarbons are discussed in some detail and rely heavily on theoretical results of Perry for the $Rh^+ + C_2H_6$ system.[27] These considerations suggest that the mechanisms of Rh^+ are quite distinct from those of Co^+, the first-row congener. This is consistent with several differences observed in the reaction behavior of these two metal ions. These differences are discussed in detail and attributed to the accessibility of the reactive s^1d^7 configuration in the case of Co^+ and the effectiveness of sd hybridization in the case of Rh^+.

Acknowledgment. P.B.A. thanks Petra van Koppen and Jason Perry for helpful discussions. This work was supported by the National Science Foundation under Grant No. CHE-9221241.

JA9509442